Linear Gaussian Kernel Cycle Generative Adversarial Networks based Transformer Learning for Early-Stage Stroke Prediction with Parkinson and Skin Disease

Dr. T. Haritha[1*], Dr.A.V.Santhosh Babu[2], Dr.B.Sharmila[3], Dr.K.Sasikala[4]

[1*]*Assistant professor , Department of computer science and technology,*

Vivekanandha college of Engineering for Women,India

[2]*Professor, Department of Information Technology, Hindusthan Institute of Technology, Coimbatore, India*

[3]*Assistant Professor, Department of Information Technology, Dr.N.G.P. Institute of Technology, Coimbatore, India*

[4]*Professor&Head,Dept.of IT, R P Sarathy Institute of Technology, India*

*1*Corresponding author email: haritha67t@gmail.com*

ABSTRACT

Stroke is the main cause of mortality and long-term disability in the whole world, and therefore, early prediction of the condition is important to enable timely medical care. Recent reports suggest that neuro-related diseases like Parkinson diseases and skin related diseases like skin wrinkles may offer reward valuable information on measuring stroke risk. Nevertheless, the current deep learning models are usually affected by difficulty in attaining high prediction accuracy and low computational time. In order to overcome these weaknesses, this paper introduces a new model of Linear Gaussian Kernel Cycle Generative Adversarial Networks-based Transformer Learning (LGKCGAN-TL) to predict strokes at an early stage. The model proposed incorporates several processing frames such as image capture, preprocessing, data augmentation, features extraction, and classification. Firstly, the pictures of Parkinson drawings and Dermnet skin disease datasets are gathered. To improve the quality of an image, the index box linear denoising technique of Camargo is used to process the image to reduce all the noise artifact and maximize the peak signal to noise ratio. This is followed by the use of Gaussian Kernel Cycle Generative Adversarial Networks (GANs) to increase the dataset and create new training samples and enhance the robustness of the model. In the case of feature learning and classification, a Rosenthal Correlative Transformer Learning model is adopted to extract geometric, texture, color, and shape features of

medical images and achieve correct stroke risk classification. There is a vast experimental assessment with such metrics as PSNR, accuracy, precision, recall, F1-score, specificity, ROC analysis, and stroke prediction time. Experimental outcomes prove that the suggested LGKCGAN-TL model reaches a higher performance of 98-99 on average prediction accuracy, 98.5 on precision, 97.8 on recall, F1-score of 98 and specificity of 93, halting the stroke prediction time to about 55 ms, which is better than other models based on GA-BiLSTM and DCNN.

Keywords: stroke disease prediction, Parkinson disease, skin wrinkles, Camargo's index box linear denoising method, Gaussian kernel cycle Generative Adversarial Networks, Rosenthal correlative transformer learning model

1. INTRODUCTION

A stroke is a Cerebrovascular diseases among the leading causes of death and disability worldwide. A stroke occurs when the blood supply to the brain is either blocked or a blood vessel in the brain bursts. It is the leading cause of death worldwide that significantly impact their quality of life. Early identification of individuals at risk is crucial for effective stroke prevention. Stroke prediction is an essential aspect of modern healthcare, aimed at identifying individuals at high risk of stroke before it occurs. Accurate prediction allows for early intervention and preventive strategies, significantly improving patient outcomes. Medical imaging plays a pivotal role in this predictive process, offering detailed insights into brain health and risk factors. Several image processing with machine learning and deep learning models has been developed for stroke prediction.

An integration of Genetic Algorithm and Bidirectional Long Short-Term Memory (GA-BiLSTM) was developed in [1] to detect strokes at an early stage through image classification by selecting the most relevant features. However, the model did not address the development of new methods for improving image quality to enhance stroke detection with minimal error. A deep convolutional neural network (DCNN) model was introduced in [2] trained with diffusion-weighted imaging to predict final acute stroke patients based on concordance correlation coefficient. But achieving minimal time consumption in stroke prediction remained a difficult task.

Artificial intelligence (AI) systems were developed in [3] to assist in categorizing, prognosing, and predicting stroke patients. However, they did not utilize advanced imaging parameters for identifying patients with stroke disease. In [4], the association between stroke and

Parkinson’s disease was analyzed. However, a deep learning model was not implemented to enhance the accuracy of disease analysis. The importance of cardiovascular and stroke risk prediction in Parkinson’s disease patients was discussed in [5] using an AI-based model. However, the approach did not significantly improve the accuracy of stroke risk prediction. A deep learning analysis technology was developed in [6] for detecting the early stages of stroke from high-definition digital images. However, predicting stroke with minimal time remains a challenging issue.

A bidirectional long short-term memory (BLSTM) model was developed in [7] for the classification of Parkinson's disease with better accuracy. However, it failed to validate its performance in analyzing the severity of stroke. An improved Attention U-Net based on 3D-CNN networks was developed in [8] to achieve accurate segmentation of 3D stroke lesions with better computational efficiency and the use of sufficient training data. However, a fast and accurate automatic segmentation solution for medical decision-making related to stroke treatment was not analyzed.

An end-to-end deep learning architecture was designed in [9] that combines information from perfusion dynamic susceptibility MRI with perfusion and diffusion parametric maps to automatically predict ischemic stroke tissue. However, the performance regarding specificity analysis remains unresolved. Logistic regressions were developed in [10] to evaluate post-stroke outcomes of patients with Parkinson's disease (PD). However, deep learning models were not applied for stroke prediction to get higher accuracy. In [11], Poststroke Parkinsonism and its association with an increased mortality risk among patients were analyzed. Cox proportional hazards regression was developed in [12] for identifying Parkinson's disease among stroke patients. However, it was not efficient for handling larger sizes of medical images to assess the risk levels of patients.

A noninvasive approach was developed in [13] for the early diagnosis of stroke, aiming to save patients' lives with minimal time consumption. However, deep feature learning from medical images remains a critical task. The Random Forest method was developed in [14] to improve the accuracy of stroke prediction datasets. However, it struggled to adequately address the outcomes of patients for early treatment of strokes and their overall survival. A deep learning model was developed in [15] for the early detection and prediction of stroke based on bioelectrical signal. But

the model failed to consider the ECG and CT scan images for better prediction and prevention of strokes.

1.1 Contributions

The novel contributions of the LGKCGAN-TL model is summarized as follows,

- To enhance stroke prediction accuracy, the LGKCGAN-TL model has been developed, incorporating preprocessing, augmentation, feature extraction, and classification.
- To improve the peak signal to noise ratio and reduce the error, LGKCGAN-TL model utilizes the Camargo's index box linear denoising method for enhancing the image quality by removing the noise.
- To minimize stroke prediction time, the LGKCGAN-TL performs the geometric features extraction using transformer learning model. With the extracted features, stroke prediction is performed, resulting in reduced prediction time.
- To improve accuracy, the Rosenthal correlative transformer learning model is employed to analyze the feature vector and provide accurate stroke prediction results.
- Finally, an experimental assessment is conducted to evaluate the performance of the LGKCGAN-TL using various metrics and comparing it to other deep learning methods.

1.2 Organization of paper

The paper is organized into the following sections: Section 2 reviews related work. Section 3 describes the LGKCGAN-TL model with a detailed diagram. Section 4 outlines the experimental setup and dataset description. Section 5 presents a comparative analysis of various metrics with different methods. Finally, Section 6 provides the overall conclusion.

2. RELATED WORKS

A multi-CNN algorithm was designed in [16] for accurate prediction of stroke outcomes using brain MRI images. However, it failed to extract and predict important clinical features necessary for accurate prediction. Facial Generative Adversarial Networks (GANs) were developed in [17] to expedite stroke detection and enhance patient triage, aiming to improve stroke treatment outcomes. However, they did not achieve optimal diagnostic performance with minimal time.

A new multimodal deep learning framework, DeepStroke, was introduced in [18] to achieve computer-aided stroke detection by analyzing patterns in minor facial muscles. However, it did not improve the efficiency of stroke detection. Automatic facial wrinkle detection algorithms were assessed using the Jaccard Similarity Index, as described in [19]. A binary logistic regression analysis was conducted in [20] for stroke prediction based on vascular risk factors. However, it did not improve accuracy and failed to effectively enhance the prediction from imaging data. A convolutional neural network (CNN)-supported segmentation and classification approach was developed in [21] to improve the accuracy of stroke prediction using deep features. However, the time consumption associated with stroke prediction was not minimized. Deep learning-based approaches were developed in [22] for brain stroke segmentation in both MRI and CT scans. However, it failed to extract high-level features for improving performance of stroke segmentation.

The Automated Deep Learning-based Brain Stroke Detection Framework (ADL-BSDF) was introduced in [23] with the aim of predicting stroke severity from MRI scans. However, it did not incorporate support for CT scan images, which could enhance stroke severity detection by localizing the stroke-affected regions in the brain. A hybrid algorithm that combines Convolutional Neural Networks (CNNs) with various machine learning algorithms was designed in [24] for the binary classification of real brain stroke CT images.

A deep learning model was developed in [25] to improve the classification of acute ischemic stroke patients based on the Dice Similarity Coefficient (DSC). However, it was not validated with a larger sample size. A 3D deep learning model was introduced in [26] with the aim of detecting acute ischemic stroke lesions. A Bayesian Convolutional Neural Network (CNN) was developed in [27] to diagnose ischemic stroke patients by incorporating Bayesian uncertainty into 2D Magnetic Resonance (MR) images. The Semantic Segmentation Guided Detector Network (SGD-Net) was introduced in [28] for accurate prediction of acute ischemic stroke from MRI images. However, it did not sufficiently address the complexity involved in predicting acute ischemic stroke. Deep learning (DL) models were developed in [29] for diagnosing stroke, aiding medical professionals in the decision-making process by extracting information from MRI data. A new deep learning approach called Early Detection of In-Sleep Stroke (EDIS) was developed in [30] by employing cascading convolutional neural networks (CNNs) to enhance both detection performance and detection time.

3. PROPOSAL METHODOLOGY

Predicting stroke involves identifying and recognizing potential lesions that lead to serious health complications if not detected promptly. Therefore, accurate and timely predicito of stroke is essential for effective treatment and management. In this paper, LGKCGAN-TL model is developed for accurate and timely prediction of stroke using Parkinson disease and skin disease. Parkinson's disease, a neurodegenerative disorder characterized by motor and cognitive impairments, and skin diseases, such as psoriasis and eczema, provide valuable insights into stroke risk. Both conditions are associated with inflammatory and systemic changes that may contribute to stroke susceptibility. The LGKCGAN-TL model integrates advanced deep learning techniques, including Generative Adversarial Networks (GANs) and Transfer Learning (TL), to analyze and interpret these complex data sources. By combining the unique features and correlations present in Parkinson's disease and skin disease data, the LGKCGAN-TL model aims to improve the accuracy of stroke prediction.

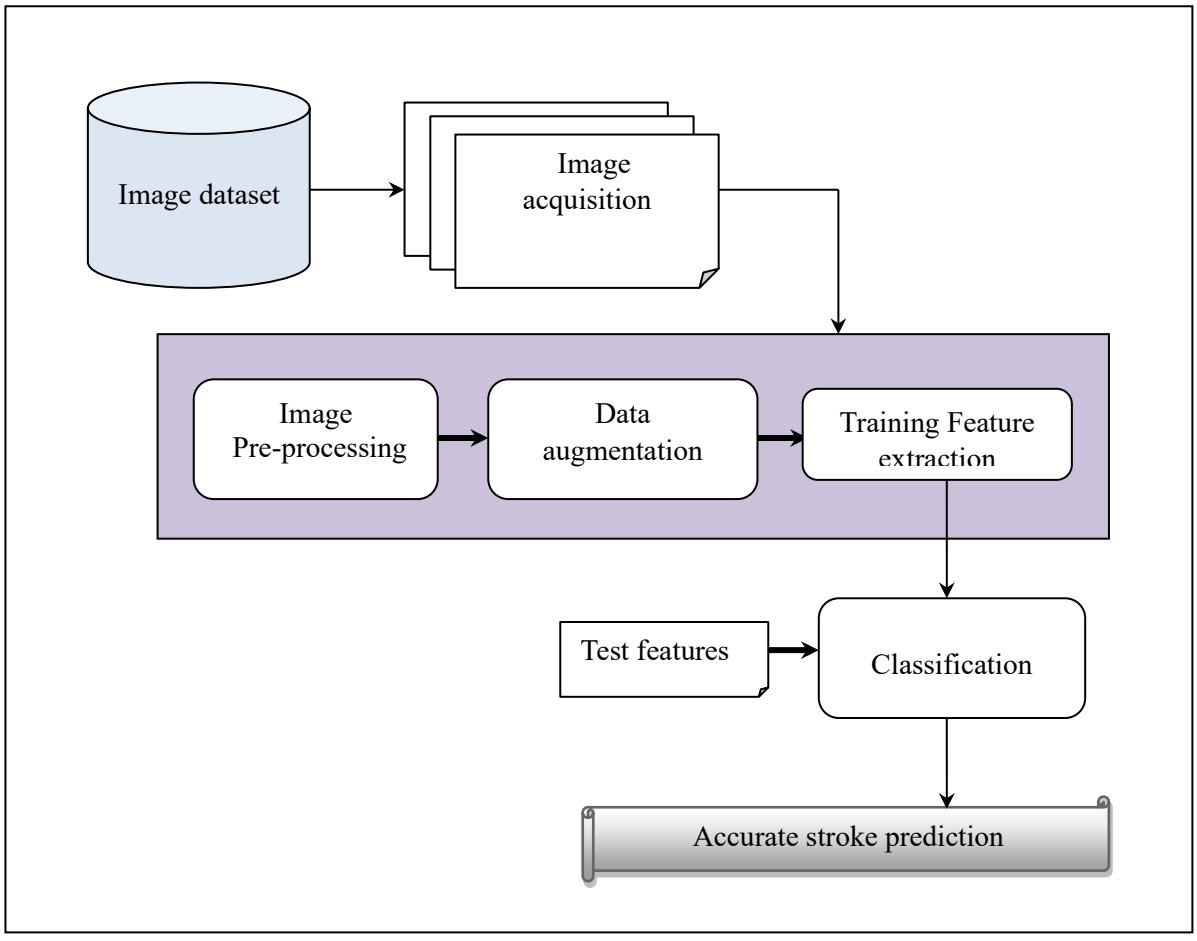


Figure 1 architecture of proposed LGKCGAN-TL model

Figure 1 illustrates the architecture diagram of the proposed LGKCGAN-TL model for accurate prediction of stroke disease at earlier stage. The accurate detection method involves five fundamental steps namely image acquisition, pre-processing, data augmentation, feature extraction and classification. These five processes of the proposed LGKCGAN-TL model are explained briefly in the following subsections.

3.1 image acquisition

Image acquisition is the process of obtaining or collecting the visual images from a dataset for further processing and analysis. In this step, the proposed LGKCGAN-TL model collects the two different types of images from the two datasets namely Parkinson disease dataset and skin wrinkle dataset for accurate stroke detection.

In order to perform the Parkinson disease, Parkinson's Drawings dataset is utilized and it taken from the https://www.kaggle.com/datasets/kmader/parkinsons-drawings .This dataset is used for distinguishing different stages of Parkinson's disease to identify the stroke patient. This dataset includes data related to drawings patterns between Parkinson's patients and healthy individuals. It consists of spiral and wave drawings collected from both groups.

The Dermnet dataset available on Kaggle [https://www.kaggle.com/datasets/shubhamgoel27/dermne] includes around 19,500 images of 23 different types of skin diseases. It is commonly used for machine learning tasks, such as the prediction of various conditions, including stroke through skin wrinkle analysis.

3.2 Camargo's index box linear denoising based image pre-processing

After the image acquisition, image pre-processing involves fundamental steps to prepare raw images into suitable format by improving the quality of the image for further analysis, such as feature extraction, and classification. It helps to improve the quality of the image and enhances the features of interest. Therefore, the proposed technique utilizes the Camargo's index box linear denoising method for improving the image quality. A box filter is a simple type of linear filter used in image processing. It works by averaging the pixel values in a specified window (box) around each pixel. This process is used for smoothing the image by reducing noise in detail. The

size of the box determines the degree of smoothing, with larger boxes leading to more significant blurring. Camargo's index is a statistical method used to enhance the performance of the box filter in the image denoising.

The main advantage of this filtering technique than the other is the uniform averaging of pixel values within the filter's window helps in reducing high-frequency noise while maintaining the overall structure of the image.

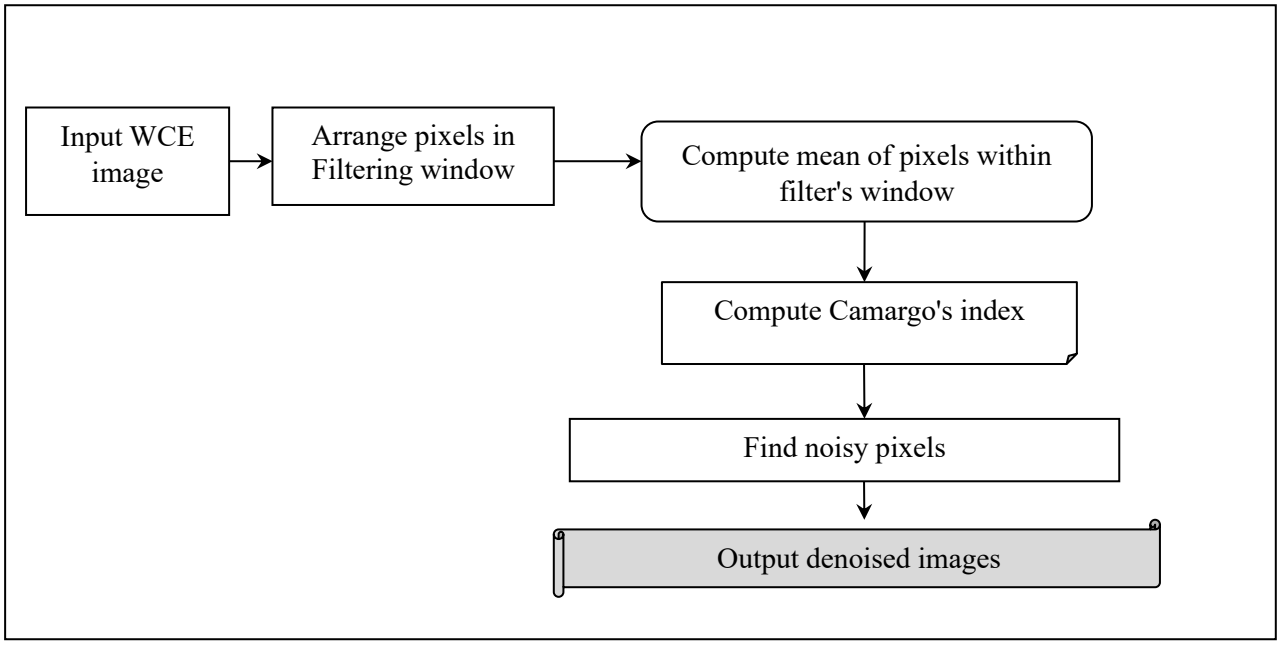


Figure 2 block diagram of the Camargo's index box linear denoising method

Figure 5 illustrates the block diagram of the image denoising for noise artifacts removal in the given input image. Let us consider the number of input image denoted as $I_1, I_2, I_3, \ldots . I_n$ taken from the two dataset Parkinson's Drawings dataset and Dermnet dataset. For each input images, the pixels are extracted and it represented by $P_1, P_2, P_3, \ldots . P_m$. Then applying the filtering technique, the pixels are arranged in the window. Therefore, the size of the filtering window is expressed as follows,

$$\mathrm{P} = \begin{bmatrix} \mathrm{P}_{11} & \mathrm{P}_{12} \ldots & \mathrm{P}_{1n} \\ \mathrm{P}_{21} & \mathrm{P}_{22} \ldots & \mathrm{P}_{2m} \\ \ldots & & \ldots \\ P_{\mathrm{m1}} & P_{\mathrm{m2}} & P_{\mathrm{mn}} \end{bmatrix} \qquad (1)$$

Where, 'P' denotes matrix where the pixels are arranged in the form of rows and columns. By considering the above matrix, compute the mean of the pixels within the filtering as given below,

$$M(P) = \frac{1}{m} \sum_{j=1}^{m} P_j \quad (2)$$

Where, $M(P)$ denotes a mean of pixels, m denotes the number of pixels. The Camargo's index is a statistical method to measure the dependency between pixel values and the mean within the filtering window. The Camargo's index function is formulated as follows,

$$S = 1 - \sum_{j=1}^{m} \frac{|P_j - M(P)|}{m} \quad (3)$$

Where, S indicates an output of Camargo's index', P_j denotes a pixel value located in the window, $M(P)$ denotes a mean of pixels,, m indicates a number of pixels. The Camargo's index function outputs values ranging from 0 to 1. Following this, the value 1 indicates normal pixel and 0 indicates a noisy pixels. In linear box filter, the noise at each pixel is replaced based on the average of its neighbouring pixels.

$$P_{filtered} = \frac{1}{k*k} \sum_{i=1}^{n} \sum_{j=1}^{m} P_{mn}(i,j) \quad (4)$$

Where, $P_{filtered}$ denotes a filtered output, $k * k$ indicates a size of the filtering window, P_{mn} indicates a pixel, i denotes a relative horizontal offset from the current pixel, j denotes a relative vertical offset from the current pixel. As a result, the quality enhanced and smoothed images are obtained for accurate stroke disease prediction. The algorithm of Camargo's index box linear denoising is described as follows,

Algorithm 1: Camargo's index box linear denoising
Input: image dataset, Number of input image $I_1, I_2, I_3, \ldots . I_n$
Output: Denoised images
Begin **Step 1**: Collect n**umber of i**nput image $I_1, I_2, I_3, \ldots . I_n$ from dataset **Step 2**: **For each** input image I_i **Step 3:** Extract the number of pixels $P_1, P_2, P_3, \ldots . P_m$ **Step 4**: Organize the pixels in filtering window

Step 5: **End for**

Step 6: Compute the mean using (2)

Step 7: Measure the Camargo's index using (3)

Step 8: **if** $(S = 1)$ **then**

Step 9: Returns noisy pixels

Step 10: **else**

Step 11: Returns normal pixels

Step 12: **end if**

Step 13: **Replace** noisy pixels using (4)

Step 14: Return (quality enhanced image)

End

Algorithm 1 outlines the process of enhancing image quality. First, images are collected from the dataset, and the pixels are positioned within a filtering window. The mean value of the pixels is calculated. Then, Camargo's index is measured to assess the dependency between pixels and the mean, distinguishing normal pixels from noise artifacts. Noise pixels are replaced with the average of neighboring pixels. Finally, the quality-enhanced image is obtained, effectively reducing the mean square error and improving the peak signal-to-noise ratio.

3.2 Image Augmentation

Image augmentation typically refers to techniques used to increase the quantity of training images from the available images. The advantage of the augmentation is to increase the dataset size and it makes the machine learning model more robust to variations. It encourages better feature learning. The proposed LGKCGAN-TL model utilizes the Cycle GAN (Cycle Consistent Generative Adversarial Network is a deep learning technique to progressively transform input image into higher-dimensional representations that resemble the target output. The Cycle GAN two crucial components such as the two generators and two discriminators which work together and it formed a ring network composed of two mirror symmetric GANs. The generator's is used to create fake images from one domain to another domain. The discriminator aims to correctly classify images as original or fake. It learns to improve its ability to distinguish between the distribution of true image and the images generated by the generator. This approach effectively generates the more number of images to perform the stroke prediction.

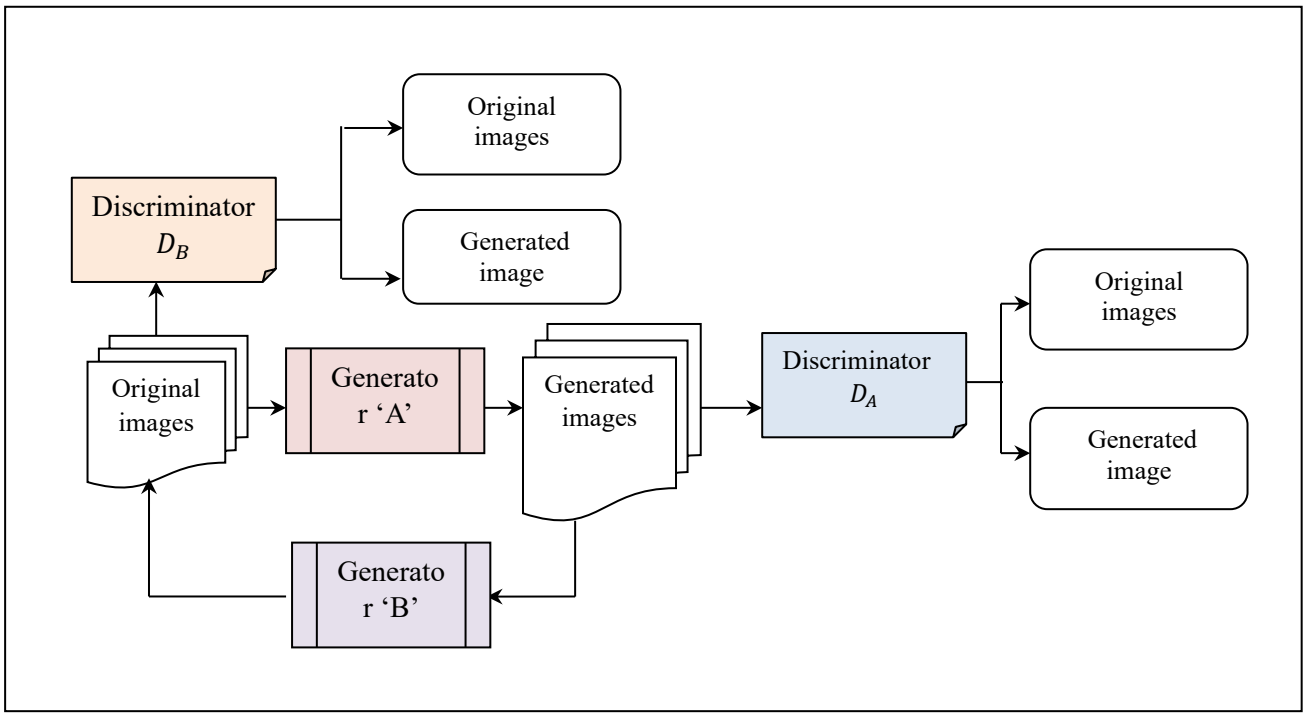


Figure 3 structure of Gaussian kernel cycle Generative Adversarial Networks

Figure 3 illustrators a structure of the cycle Generative Adversarial Networks for generating the large volume of images from the input images. The Cycle GAN two crucial components such as the two generators A and B and two discriminators 'D_A' and 'D_B' which work together and it formed a ring network. The network considers the preprocessed input images $I_1, I_2, I_3, \ldots . I_n$ are taken as input and it given to the Generator 'A'. The generator progressively increases the spatial dimensions of the input images. This process is essential for transforming a low-dimensional vector into high-dimensional synthetic images. The equations for generator 'A' are expressed as follows,

$$I_S = G_A(I) \quad (5)$$

Where 'I' represents an image from domain input domain, I_S denotes the generated image in another domain through generator G_A for transforming images from I to I_S. The newly generated mage with pixels of the input image is expressed as follows,

$$P_G = \sum_{j=1}^{m} P_j * K \quad (6)$$

Where,

$$K = \frac{1}{\sqrt{2\pi\sigma^2}} \exp\left(-0.5 \frac{|P_j - \mu|}{\sigma^2}\right) \quad (7)$$

Where, P_G denotes a newly generated pixels of the particular image, P_j denotes an already available image pixels in the image, K indicates a Gaussian kernel, μ denotes a mean of all available pixels in the image, σ indicates a standard deviation. In this way, new pixels of the images are generated from the already available pixels in the input image. The output of the generator is now a set of pixel values and it arranged in a grid to form an image. Each pixel in this grid is determined by the features learned by the generator during training. These features include edges, textures and shapes.

Then the output of generator is given to the discriminator 'D_A' and distinguishes the original and generated images through the similarity measure between the pixel values in original images and generated images. Hamann index function statistical technique is used for estimating the similarity between the pixels as follows

$$HS = 1 - \frac{2|P_O \Delta P_G|}{n} \quad (8)$$

Where, HS denotes a Hamann similarity, P_O denotes pixels in original image, P_G denotes a pixels in generated images, 'n denotes a number of pixels, $P_O \Delta P_G$ denotes a variation between the two pixels. Based on the pixels analysis, the similarity 'HS' returns a value from 0 to 1.

$$HS = \begin{cases} 1 \; ; & original\ image \\ 0 \; ; & generated\ image \end{cases} \quad (9)$$

From the analysis, discriminator 'D_A' classified the generated picture represented by 0, and the original image represented by 1.

Then the generator 'B' is used for transforming images from domain I_S to I in a CycleGAN which represented by the following equation,

$$I = G_B(I_S) \quad (10)$$

Where, generator G_B responsible for transforming images from I_S to I. The above said generator process is used for creating the synthetic images. After that, the discriminator 'D_B' distinguishes the original images and generated images. Based on the learning process, two types

of losses are measured such as adversarial loss and cycle consistency loss. The proposed method reduces the loss between the generated and original images.

The adversarial loss of the generators discriminators is measured as follows,

$$L_{al} = E_{I_S \sim pimage(I_S)} [\log D_B(I_s)] + E_{I \sim p\ image(I)} [\log(1 - D_B(G_A(I))] \quad (11)$$

Where, L_{al} denotes a adversarial loss , $E_{I_S \sim pimage(I_S)}$ denotes a expected value of the log of the discriminator's output for generated image I_S' sampled from the true probability distribution $pimage(I_S)$, $D_B(I_s)$ discriminator outcome for generated images, $E_{I \sim p\ image(I)}$ denotes a expected value of the log of the discriminator's output for generated original image, $D_B(G_A(I)$ indicates a discriminator's output for original image.

Cycle consistency loss is used to translate images from one domain to another and then back again, ensuring that the original image is preserved through this cycle of transformations. It is formulated as follows,

$$L_{cc} = E_{I \sim pimage(I)} \|I_S - I\|_1 \quad (12)$$

Where, L_{cc} denotes a Cycle consistency loss, $E_{I \sim p\ image(I)}$ denotes a expected value of the log of the discriminator's output for generated original image, I_S denotes a reconstructed image, I denotes a original image, $\| \quad \|_1$ denotes a L1 norm to calculate the loss between the reconstructed image and the original image. The cycle consistency loss ensures that the learned mappings generator and discriminator consistent with each other. By minimizing this loss, the model is better to learn meaningful transformations between the two domains, preserving the essential structure and content of the original images through the translation cycles.

// Algorithm 2: Gaussian kernel cycle Generative Adversarial Networks based image augmentation
Input: Preprocessed input image
Output: Generate more input images
Begin **Step 1**: **Collect** number of preprocessed images **Step 2:** Give input to generator ''G_A'

Step 3: **for each** image I

Step 4: Generate the new images using (6) (7)

Step 5: Given trainings images to Discriminator 'D_A'

Step 6: Measure the pixel similarity using (8)

Step 7: ***if*** $(HS = 1)$ **then**

Step 8: classified as original image

Step 9: **else**

Step 10: classified as generated image

Step 11: **End if**

Step 12: End for

Step 13: Repeat step from 3 to 12 for generator 'G_A' and Discriminator 'D_A'

Step 14: Obtain (more generated images)

End

Algorithm 2 outlines the process of image augmentation using Gaussian Kernel Cycle Generative Adversarial Networks (GANs). The augmentation process begins with preprocessed images as input. The Generator uses the Gaussian kernel function to generate new pixels based on the existing pixels of the given image. Subsequently, the discriminator evaluates both the original image and the generated image. This process is repeated with a second Generator and Discriminator. Thus, the proposed Gaussian Kernel Cycle GAN effectively generates synthetic images by minimizing both the adversarial loss and the cycle consistency loss.

3.4 Rosenthal correlative transformer learning based classification

The Transformer learning is a deep learning model architecture that utilizes the transformer framework for stroke prediction though the Parkinson disease and skin disease. On contrary to traditional deep neural networks, the Transformer learning utilizes self-attention mechanisms to measure the relationships between different patches of an image. This approach helps the model to efficiently handle long-range dependencies and capture global features for accurate disease classification. By dividing an image into a sequence of patches in parallel, the transformer learning model achieves improved performance especially the size of the image samples increases. This novel contribution of transformer models enhances the efficiency of disease detection.

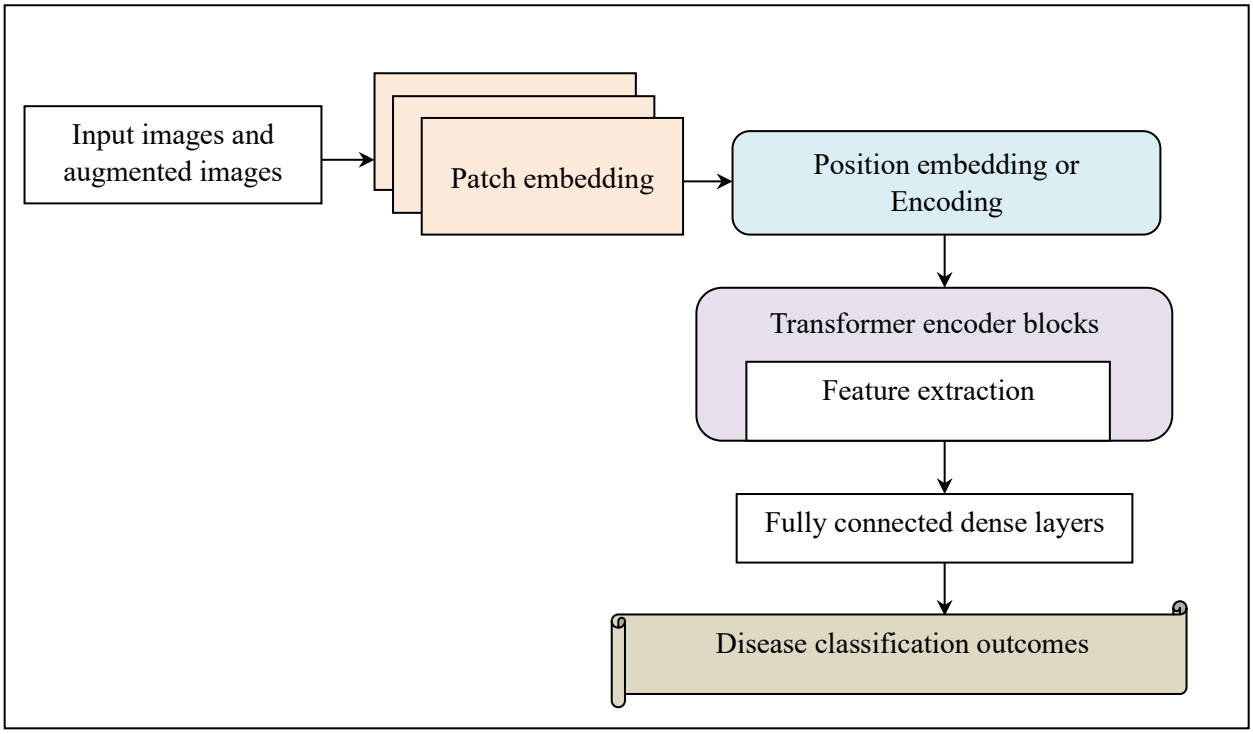


Figure 4 flow process of Rosenthal correlative transformer learning based classification

Figure 4 depicts the flow process of transform learning network used for feature learning and disease classification. The Transformer learning network includes four processes namely patch embedding, positional encoding, transformer encoder, and classification head. First, the patch embedding is employed to divide the input image into fixed-size non-overlapping patches. Second, positional encoding is performed to arrange the position of each patch. Followed by, the results of embeddings are transferred to Transformer encoder layers. Each layer consists of self-attention network and feed-forward networks, enabling the model to capture both local and global features such as shape, size, and texture within the images. Finally, the extracted features are combined in the feature fusion process. These results are given to the fully connected dense network for classifying the input images into different classes.

3.4.1 Patch embedding

Patch embedding is a fundamental concept in Transformers learning that handle images by dividing them into patches. It involves transforming image patches into a suitable format for further processing. In order to perform patch embedding, the input images '*I*' first splits into different patches with similar sizes

$$I \in R^{H*W*C} \qquad (13)$$

Where, R^{H*W*C} indicates a patches with similar height 'H', width 'W' and channel (RGB) 'C'. The linear transformation process is used for converting a patch matrix into a column vector

$$A = \begin{bmatrix} P_{11} & P_{12} & \dots & P_{1n} \\ P_{21} & P_{22} & \dots & P_{2n} \\ \vdots & \vdots & \vdots & \vdots \\ P_{m1} & P_{m2} & \dots & P_{mn} \end{bmatrix} \quad (14)$$

The linear transformation process is then flattened into a one-dimensional vector.

$$A \xrightarrow{LT} R_k \quad (15)$$

Where, A denotes a patch matrix with number of pixels in input image, LT indicates a linear transform, R_k denotes a column vector

$$R_k = \begin{bmatrix} P_{11} \\ P_{21} \\ \vdots \\ P_{m1} \\ P_{12} \\ \vdots \\ P_{m2} \\ \vdots \\ P_{mn} \end{bmatrix} \begin{matrix} \} \\ \\ \\ \\ \} \\ \\ \\ \\ \} \end{matrix} \begin{matrix} R_1 \\ \\ \\ \\ R_2 \\ \\ \\ \\ R_k \end{matrix} \quad (16)$$

$$R_k = [R_1, R_2, R_3, \dots R_k] \quad (17)$$

Where, R_k denotes a number of patches $R_1, R_2, R_3, \dots R_k$ of images.

3.4.2 Positional embedding

Positional embedding is a technique used in transformer models to incorporate information about the position in a sequence based pixel values in patches of an image. Positional encoding process is expressed as follows,

$$Q_E(b, 2_r) = \sin\left(\frac{b}{W^{\left(\frac{2r}{d}\right)}}\right) \quad (18)$$

$$Q_E(b, 2_{r+1}) = \cos\left(\frac{b}{W^{\left(\frac{2r}{d}\right)}}\right) \quad (19)$$

Where, Q_E denotes a position embedding, b indicates a length of patch sequence starts from 1 to $N-1$, where N denotes total number of patches in the sequence, d represents the

dimensionality of the embedding size, $Q_E(b, 2_r)$ symbolizes the r^{th} dimension of the embedding for the position 'b' with a sine function, $Q_E(b, 2_{r+1})$ indicates the r^{th} dimension of the positional embedding for the position 'b' with a cosine function, W denotes user-defined scalar term (i.e. 10,000).

3.4.3. Transformer encoder layers

The Transformer encoder layers are used for processing and transforming input data into a suitable format to make predictions or classifications. The position embedding output is passed into the Transformer encoder layers. These layers include a self-attention network and feed-forward networks, which allow the model to capture image features like shape, size, and texture. The self-attention mechanism enables the model to concentrate on the most relevant parts of the input images.

Texture features are used to quantify the spatial patterns and structures within an image. These features are essential in medical imaging.

$$F_{TX} = \frac{\sum_j \sum_n (PI_j - \mu_j)(PI_n - \mu_n).P_r(PI_j, PI_n)}{v_j.v_n} \quad (20)$$

Where, F_{TX} denotes a texture feature between the pixel intensity 'PI_j' and its neighboring pixels intensity 'PI_n', μ_j and μ_n denotes a mean intensities of pixels PI_j and PI_n, $v_j.v_n$ denotes a deviation.

The colour features are extracted to describe the overall colour tone and variation in an image. The mean and standard deviation of colour channels are fundamental for each colour channel (e.g., red, green, and blue in RGB images) and it provide insights into the image's colour distribution and contrast.

$$\mu = \frac{1}{m} \sum_{j=1}^{m} PI_j \quad (21)$$

Where, μ indicates a mean, PI_j denoting a pixel intensity. The deviation measures the amount of variation of pixel intensities from the mean. It provides information about the contrast and variability in the image.

$$v = \sqrt{\frac{1}{m} \sum_{j=1}^{m} (PI_j - \mu)^2} \quad (22)$$

Where,v denotes a deviation, PI_j denoting a pixel intensity, μ denotes a mean, m denotes a number of pixel intensity.

The shape feature is extracted based on perimeter which measured by counting the number of boundary pixels in border. The perimeter is the length of the boundary of the object. The distance between consecutive points within the boundary is measured as follows,

$$B = \sum_{j=1}^{m} \sqrt{(p_{j+1} - p_j)^2 + (q_{j+1} - q_j)^2} \quad (23)$$

Where, B denotes a perimeter, (p_j, q_j) are the coordinates of the j^{th}boundary pixels, and (p_{j+1}, q_{j+1}) indicates the coordinates of consecutive boundary pixel. It helps to known that shapes of object. These extracted feature vector is passed to fully connected dense layer for classification of disease

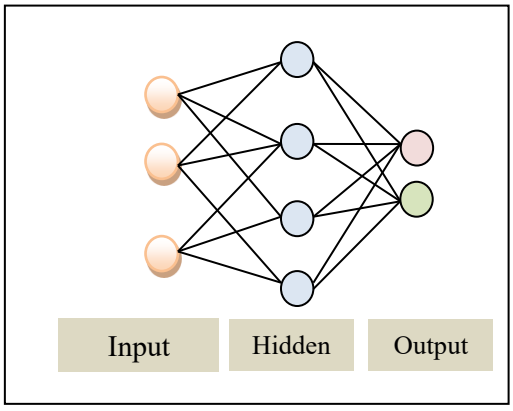


Figure 5 Structure of fully connected dense layer

Figure 5 indicates the structure of fully connected dense layer which includes layers, input layer, hidden layer, and an output layer. The input layer consists of nodes (neurons) that received the extracted features. Each hidden layer consists of multiple nodes, and performs the certain task. The output layer consists of nodes based on number of labels in the dataset.

Each neuron in the input layer received the input and it assigns a corresponding weights and the bias.

$$Z = \sum(EFV * w) + g \quad (24)$$

Where,Z denotes an activity of the neuron in the input layer, EFV denotes an extracted feature vector from the Parkinson dataset and skin disease dataset, w denotes weights assigned to

an input. 'g' indicates a bias that stored the value is '1'. Then the input is transferred into the hidden layer where the feature analysis is performed. In that layer, the testing and training features i.e. extracted feature vector from these two images are analyzed by applying Rosenthal correlation function. The correlation between the features is measured as follows,

$$RC\ (EFV, TFV) = \left[\frac{WST}{\sqrt{k}}\right] \quad (25)$$

Where, $RC\ (EFV, TFV)$ indicates a Rosenthal correlation between the extracted feature vector 'EFV' and testing feature vector 'TFV', WST denotes a Wald Standardized test statistics, k' indicates the number of features vector.

$$WSS = \frac{(EFV-TFV)^2}{var(EFV,TFV)} (26)$$

Where, $var(EFV, TFV)$ denotes a variance between the features. The output of statistical outcome is then passed through an activation function.

$$Y = F_s[\ RC\ (EFV, TFV)] \quad (27)$$

$$F_S = [1 + \exp(-RC\ (EFV, TFV)]^{-1} (28)$$

Where, φ_S denotes a sigmoid activation function, TS denotes a test statistics outcomes. The sigmoid activation function provides the output probabilities as either 0 or 1.

If the testing and training features in a Parkinson's disease dataset are matched, this may help identify patients who are at risk of stroke, indicated by '1'. The inflammation associated with Parkinson's disease may contribute to vascular damage, potentially increasing the risk of stroke.

In case of skin disease, Psoriasis, Severe Eczema, and Lupus are used for inflammatory skin conditions that may have systemic implications, including potential contributions to stroke risk. Patients with psoriasis often have higher rates of cardiovascular diseases, such as hypertension, and diabetes, all of which are risk factors for stroke. Severe Eczema is linked to increased stress and sleep disturbances, which intensify cardiovascular risk factors like hypertension, potentially leading to stroke. Lupus is particularly associated with a high risk of cardiovascular complications, including stroke. Through the output of the Transformer learning model, patient's stroke severity risk levels is effectively classified. Therefore, the proposed Transformer learning approach enhances the performance of stroke disease prediction while minimizing time consumption. The algorithm of is described as give below,

//Algorithm 3: Rosenthal correlative transformer learning based classification
Input: **input** images '$I = \{I_1, I_2, \dots, I_h\}$'
Output: Increase the accuracy of disease prediction
Begin
Step 1: Collect number of images '$I = \{I_1, I_2, \dots, I_h\}$ '
Step 2: **For each** image 'I
Step 3: Perform patch embedding using (17)
Step 4: Perform position embedding using (18) (19)
Step 5: **End for**
Step 6: Transform position embedding matrix into transformer layers
Step 7: Extract feature vectors from patches
Step 8: **Transform the extracted** fusion feature vector into fully connected dense layer
Step 9: **For each feature** vector EFV and TFV
Step 10: Measure correlation using (25)
Step 11: **End for**
Step 12: Apply sigmoid activation function using (28)
Step 13: **If** '$F_S = 1$' **then**
Step 14: classified into increase the risk of stroke
Step 15: **else**
Step 16: classified into minimize the risk of stroke
Step 17: **End if**
Step 18: Obtain final classification results **------(output layer)**
End

Algorithm 3 outlines a process for stroke disease risk prediction. Initially, a set of sample images is provided as input to the Transformer learning network. For each image, the patch embedding process is performed, partitioning the input image into multiple patches of equal size. Next, the position embedding process is conducted to arrange the sequential order of patches, preserving the spatial relationships within the images. The resulting position embeddings are then fed into the transformer layers. In these layers, the dimensionality of the input image is reduced by

extracting significant feature vectors. These fused feature vectors are then transferred to the fully connected dense layer network. Within this network, Rosenthal correlation is applied in the hidden layer to analyze the relationship between the extracted feature vectors and the testing features. Based on this analysis, the sigmoid activation function in the output layer provides the final prediction, indicating the likelihood of stroke risk. As a result, accurate stroke risk prediction is achieved with minimal error.

4. EXPERIMENTAL SETUP

An experimental assessment of the proposed LGKCGAN-TL model and existing GA-BiLSTM [1], DCNN [2] is implanted in python programming language for accurate stroke risk prediction based on two image datasets namely Parkinson's Drawings dataset https://www.kaggle.com/datasets/kmader/parkinsons-drawings and Dermnet dataset https://www.kaggle.com/datasets/shubhamgoel27/dermnet . Table 1 presents the implementation parameters.

Table 1: Implementation Parameters of the Proposed LGKCGAN-TL Model

Parameter	Value
Programming Language	Python
Deep Learning Framework	TensorFlow / PyTorch
Hardware Environment	Intel i7 Processor, 16 GB RAM, NVIDIA GPU
Operating System	Windows / Linux
Image Format	JPEG
Image Channels	RGB (3 channels)
Image Resolution	224 × 224 pixels
Parkinson Dataset Size	72 images (36 healthy + 36 Parkinson)
Dermnet Dataset Size	19,500 images (used classes: Psoriasis, Eczema, Lupus)

Selected Dermnet Images	766 images
Augmented Dataset Size	Up to 1000 images
Noise Removal Technique	Camargo's Index Box Linear Denoising
Patch Size (Transformer)	16 × 16
Transformer Layers	12
Attention Heads	8
Activation Function	Sigmoid
Learning Rate	0.001
Batch Size	32
Training Epochs	50
Loss Function	Binary Cross-Entropy
Train–Test Split	80% Training – 20% Testing

4.1 Dataset description

This Parkinson's Drawings dataset is used for distinguishing different stages of Parkinson's disease to identify the stroke patient due to the drastic changes in the patterns of the spiral test. This dataset includes of 36 healthy and 36 patients with Parkinsons drawing spirals out of a 72 training Drawings images.

The Dermnet dataset includes around 19,500 images of 23 different types of skin diseases. Among these, three types of diseases are particularly influential in increasing the risk of stroke such as Psoriasis, Eczema, and Lupus. The images are in JPEG format, consisting of 3 channels (RGB). The resolutions vary from image to image and from category to category. The dataset includes 309 images for Psoriasis, 105 images for Eczema, and 352 images for Lupus.

To perform data augmentation, the sizes of all dataset images are increased to 1000. For experimental purposes, the number of images is varied from 100 to 1000.

4.2 Sample Outcomes of Dataset Processing Pipeline

This section presents the sample outcomes of the proposed processing pipeline applied to two different datasets used in this study: the Parkinson's Drawings dataset and the DermNet skin disease dataset.

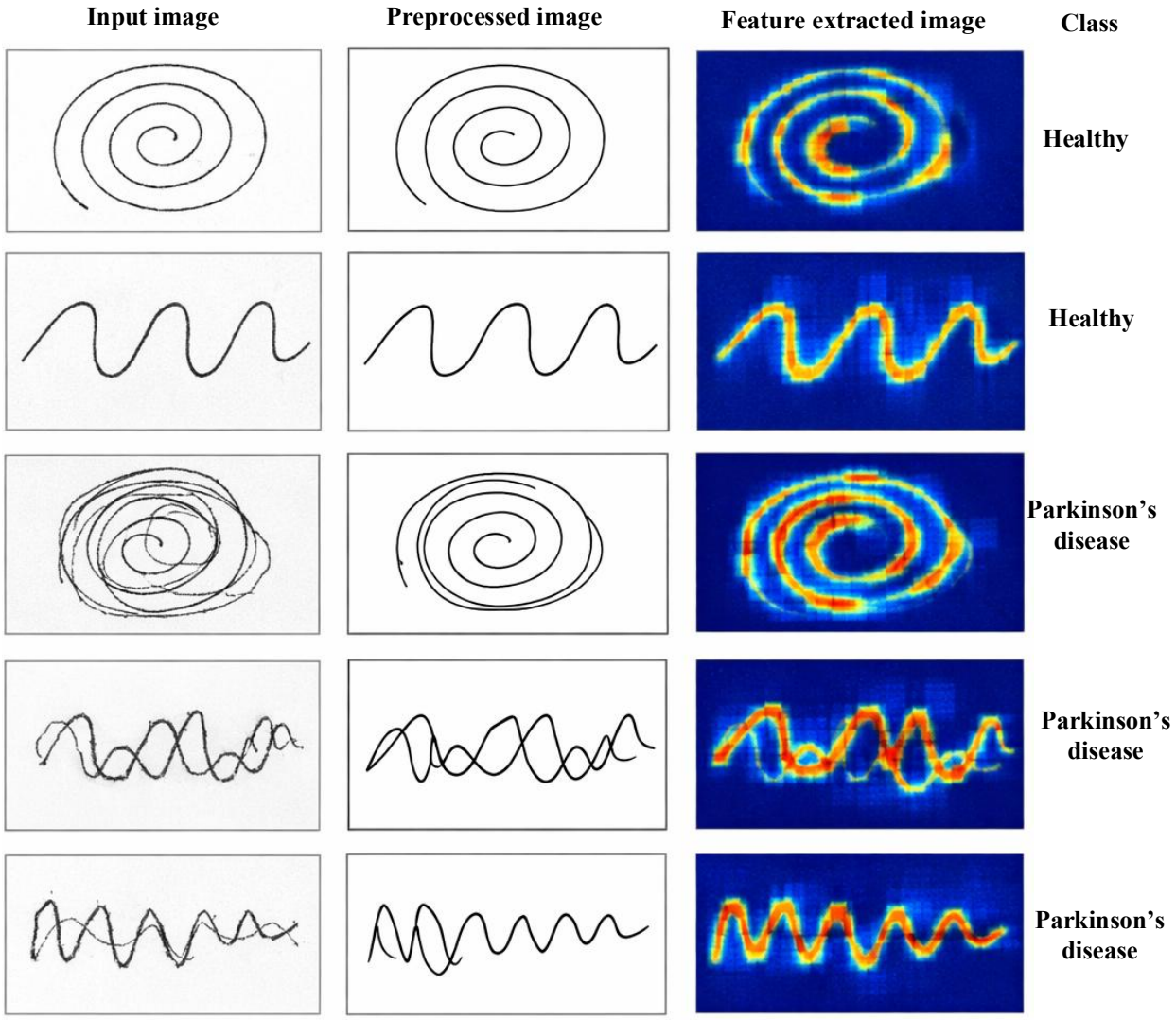


Figure 6: Sample Outcome of Parkinson's Drawings Dataset Processing Pipeline

The figure 6 shows a sample results on the Parkinson's Drawings dataset on the processing pipeline of classifying the disease. The original input images in the form of spiral and wave drawings that were made by subjects are presented in the first column. The second column shows the preprocessed images in which noise elimination, normalization and smoothing of the images is implemented to improve drawing patterns. The third column is the extracted feature images with

discriminative texture and structural features identified in a heatmap format. The last column denotes the respective labels of the classes with the determination of the individuals who are healthy and those with Parkinson disease. Distorted, irregular and tremor affected patterns can be observed in the drawing of Parkinson as compared to more smooth patterns in normal samples.

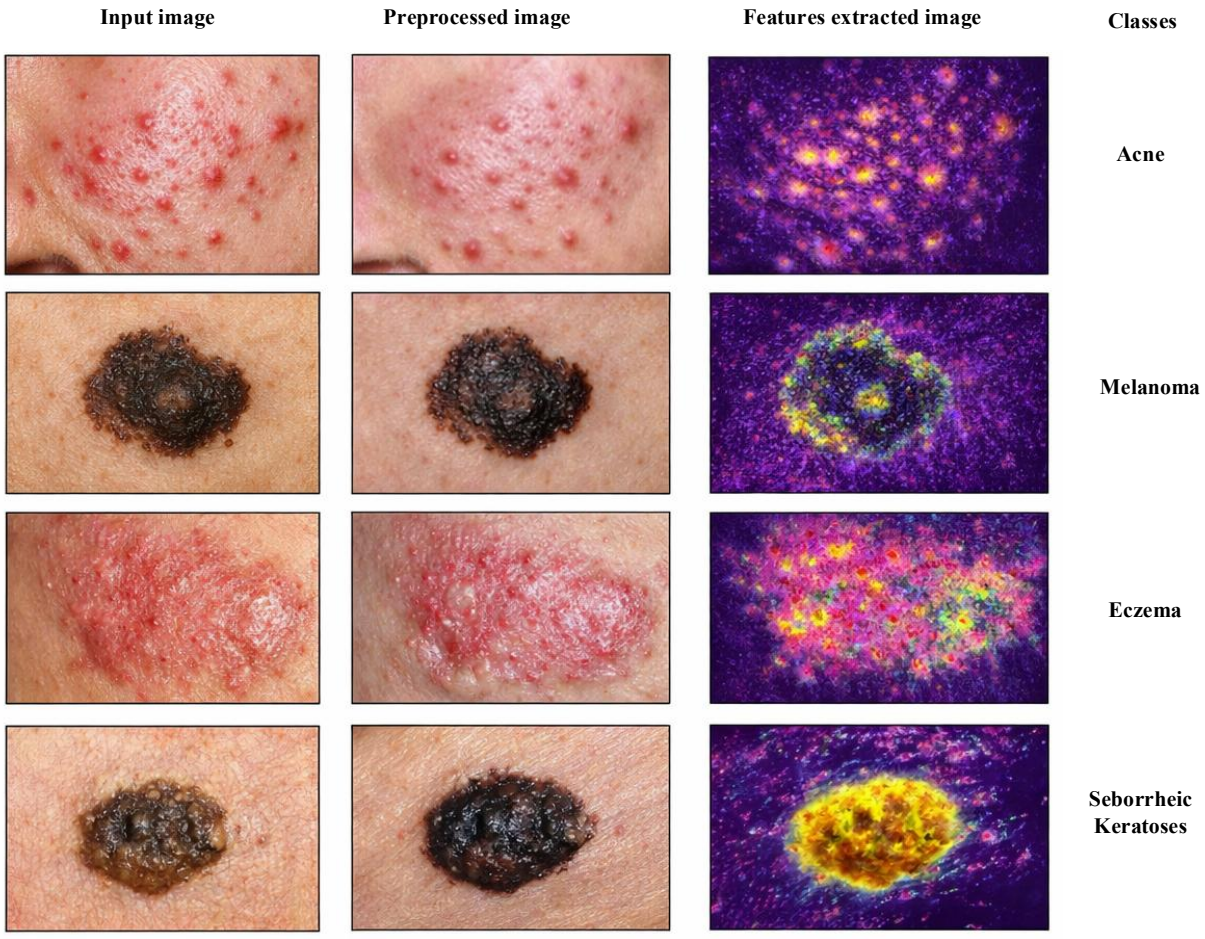


Figure 7: Sample Outcome of DermNet Dataset Processing Pipeline

The figure 7 shows the sample result of the DermNet skin disease dataset processing line applied in the suggested model. The rows denote the various dermatological diseases among them being Acne, Melanoma, Eczema, Seborrheic Keratoses, Tinea Ringworm, Bullous Disease, Poison Ivy, Psoriasis, and Vascular Tumors. The original dermoscopic image of the dataset is displayed in the first column. The second column shows the processed image of the removal of noise, resizing, and normalization to improve visualization. The third column shows the extracted feature representation of the important patterns and textures in the image used to ascertain classification.

The last column is the expected missing class of the disease produced by the trained deep learning model to successfully identify the skin disease.

5. PERFORMANCE ANALYSIS

In this section, the performance analysis of the LGKCGAN-TL model and existing GA-BiLSTM [1], DCNN [2] are compared with various metrics. The metrics involved for evaluating the performance of proposed LGKCGAN-TL model such as peak signal to noise ratio, accuracy, precision, sensitivity, specificity and stroke prediction time, confusion matrix and ROC curve.

Peak signal to noise ratio**:** It is used to evaluate the quality of a preprocessed image, by comparing it to the original image. The Peak signal to noise ratio is calculated based on mean squared error (MSE) between the original and preprocessed image.

$$PSNR = 10 * \log_{10}\left[\frac{{P_{max}}^2}{\text{MSE}}\right] \quad (29)$$

$$\text{MSE} = [I_{size} - \text{Pr}(I)_{size}\,]^2 \quad (30)$$

Where '$PSNR$' indicates a peak signal to noise ratio, 'P_{max}' represents the maximum possible pixel value (255), MSE indicates a mean square error,$\text{Pr}(I)_{size}$ indicates preprocessed image size, I_{size} denotes original image size. It is expressed in decibels (dB).

Accuracy: it refers to the ability of a model to correctly identify whether a images sample cause the risk of stroke or not. It is typically evaluated as follows,

$$Acc = \frac{TP+TN}{TP+TN+FP+TN} \quad (31)$$

Here, 'Acc' denotes accuracy, where true positive rate (TP) refers to the correct prediction of images as stroke, false negative rate (FN) refers to the incorrect prediction of stroke images as normal, false positive rate (FP) refers to the incorrect prediction of normal images as stroke, and true negative rate (TN) refers to the correct identification of normal images.

Precision: Precision is a metric used to evaluate the accuracy of positive predictions made by a model. It specifically measures the proportion of true positive predictions out of all the positive predictions. It is calculated as:

$$Precision = \frac{TP}{TP+FP} \quad (32)$$

Where, precision is measured with the aid of the true positive rate 'TP' and false positive rate 'FP'.

Recall: it, also known as sensitivity is a metric used to evaluate the ability of a model to identify all relevant positive cases in a dataset. It measures the proportion of actual positive cases that are correctly identified by the model.

$$Recall = \frac{TP}{TP+FN} \quad (33)$$

Where, recall is measured with the aid of the true positive rate 'TP' and false negative rate 'FN'.

F1-score: It is a metric that combines precision and recall into a single value to provide a balanced assessment of a model's performance. It is the harmonic mean of precision and recall.

$$F1\ score = 2 * \left(\frac{precision*Recall}{Pprecision+Recall}\right) \quad (34)$$

Specificity: it measures the proportion of actual negative cases that are correctly identified by a classification model. It reflects the model's ability to correctly identify negative instances.

$$Specificity = \frac{TN}{TN+FP} \quad (35)$$

Where, Specificity is measured with the aid of the true negative 'TN' and false positive rate 'FP'.

Stroke prediction time: It is defined as the amount of time taken by the algorithm to perform stroke prediction in the given input image. The overall time consumption is formulated as follows,

$$SPT = \sum_{i=1}^{h} I_i * Time\ [(SP)] \quad (36)$$

Where 'SPTindicates a stroke prediction time, h denotes the number of image samples 'I', $Time\ (SP)$ denotes a time for prediction of stroke. It is measured in milliseconds (ms).

Table 2 peak signal to noise ratio using Parkinson's Drawings dataset

Image size (KB)	Peak signal to noise ratio (dB)		
	LGKCGAN-TL	GA-BiLSTM	DCNN
72.78	65.85	60.89	57.76
78.59	60.52	54.68	52.71
77.44	62.55	56.30	53.32
69.53	63.52	59.18	53.97

73.35	60.89	57.24	54.87
75.25	62.11	57	51.35
74.7	55.06	51.87	49.96
76.02	65.85	60.52	54.87
71.14	65.20	60.17	55.06
68.92	56.53	52.56	49.34

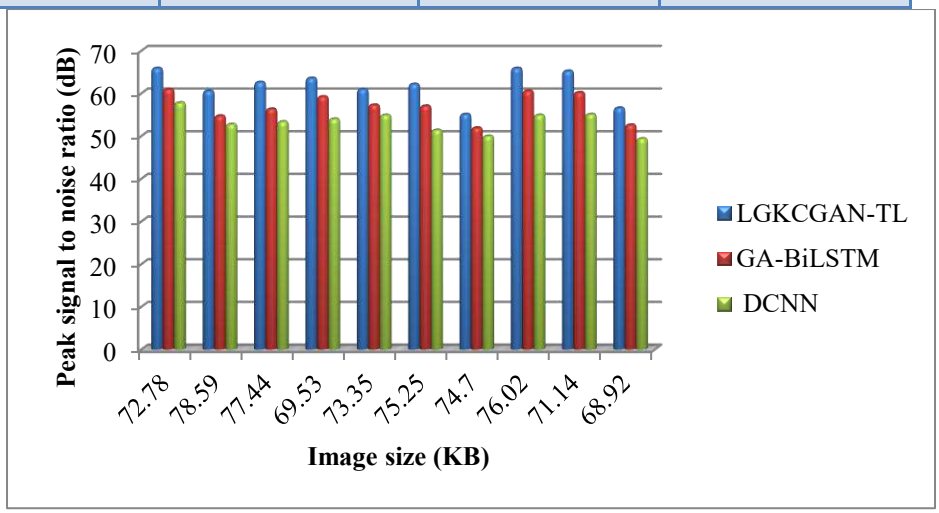


Figure 8 performance results of peak signal to nose ratio using Parkinson's Drawings dataset

Table 3 peak signal to noise ratio using Dermnet dataset

Image size (KB)	Peak signal to noise ratio (dB)		
	LGKCGAN-TL	**GA-BiLSTM**	**DCNN**
82.51	64.60	58.88	54.87
57.49	59.50	54.32	52.56
83.80	60.17	53.32	51.87
91.62	56.08	53.01	52.28
81.53	58.30	52	48.39
86.21	64.04	61.68	55.46
85.66	58.58	55.26	51.73
77.95	54.15	50.62	48.57
82.36	58.30	50.06	47.06
86.15	64.60	59.83	52.71

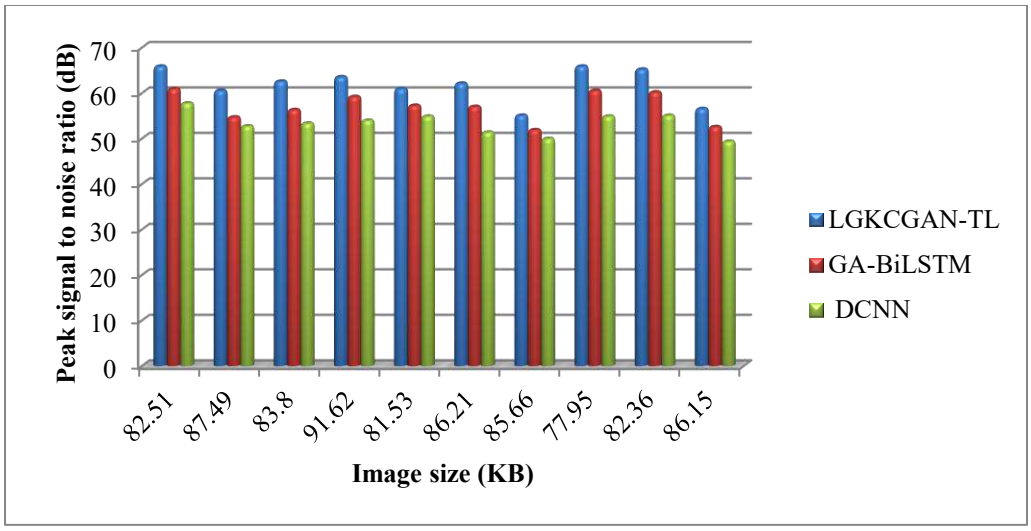


Figure 9 performance results of peak signal to nose ratio using Dermnet dataset

Figure 8 depicts the performance outcomes of peak signal-to-noise ratio (PSNR) with respect to different sizes of input images, measured in kilobytes (KB), taken from the Parkinson's Drawings dataset. Figure 9 shows the performance outcomes of PSNR with respect to different sizes of input images, also measured in kilobytes (KB), taken from the Dermnet dataset. The PSNR is measured using three methods: the LGKCGAN-TL model, the existing GA-BiLSTM [1], and DCNN [2]. As illustrated in Figures 8 and 9, the LGKCGAN-TL model demonstrates improved performance in PSNR analysis compared to the existing methods. This improvement is attributed to the proposed LGKCGAN-TL model, which utilizes Camargo's index box linear denoising method to identify and correct noisy pixels in the input images. The pixels in the input images are positioned within a filtering window, and the mean value of these pixels is calculated. Camargo's index is then evaluated to measure the dependency between the pixels and the mean value. Based on this dependency measure, normal pixels are differentiated from noise. The noisy pixels are replaced with the average of neighboring pixels within the filtering window, resulting in enhanced image quality by reducing the mean square error and improving the PSNR. For each method, various results were observed and compared. By using the Parkinson's Drawings dataset, the average of ten comparisons showed that the PSNR improved by 8% and 16% using the LGKCGAN-TL model compared to [1] and [2], respectively. Similarly, using the Dermnet dataset, the average performance of PSNR improved by 9% and 16% using the LGKCGAN-TL model compared to [1] and [2], respectively

Table 4 Accuracy

Number of images	Accuracy using Parkinson's Drawings dataset			Accuracy using Dermnet dataset		
	LGKCGAN-TL	GA-BiLSTM	DCNN	LGKCGAN-TL	GA-BiLSTM	DCNN
100	0.98	0.93	0.91	0.97	0.93	0.90
200	0.982	0.935	0.916	0.972	0.922	0.915
300	0.972	0.932	0.905	0.970	0.93	0.9
400	0.982	0.942	0.914	0.980	0.924	0.904
500	0.99	0.933	0.90	0.973	0.930	0.912
600	0.980	0.925	0.894	0.962	0.937	0.9
700	0.982	0.934	0.906	0.967	0.924	0.894
800	0.979	0.93	0.9	0.970	0.927	0.893
900	0.983	0.94	0.912	0.974	0.935	0.904
1000	0.98	0.93	0.91	0.97	0.927	0.894

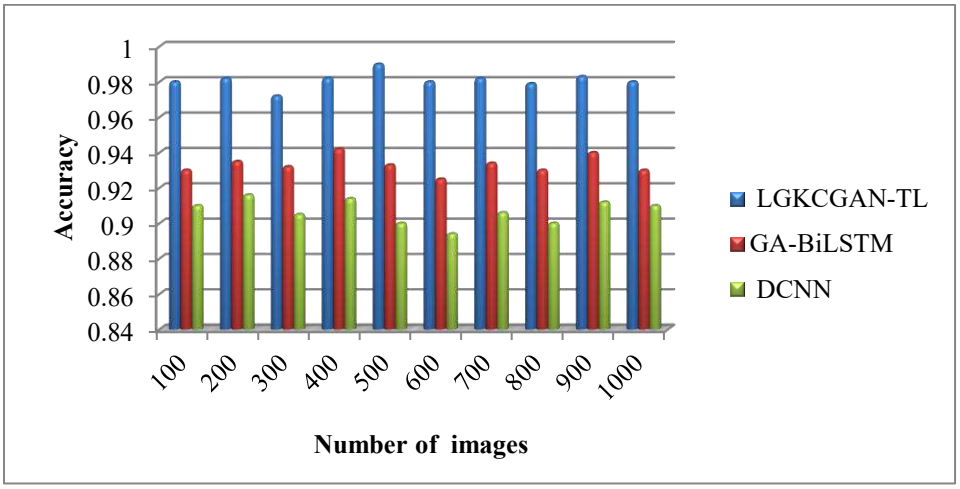


Figure 10 performance results of accuracy using Parkinson's Drawings dataset

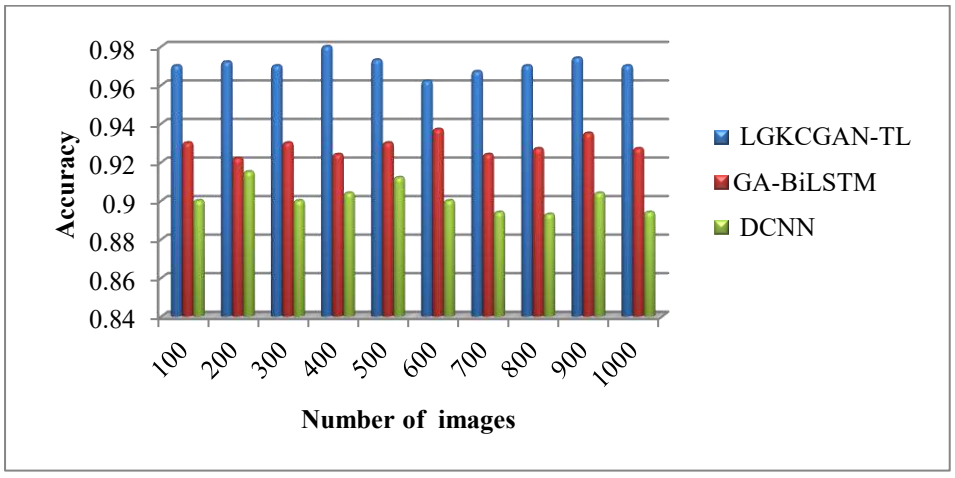


Figure 11 performance results of accuracy using Dermnet dataset

Figure 10 and 11 demonstrates a performance outcomes of stroke prediction accuracy versus the number of images, ranging from 100 to 1000 collected from the Parkinson's Drawings dataset and Dermnet dataset. The numbers of images are taken in horizontal axis and the accuracy was observed on the vertical axis. The graphically analyzed result shows that the accuracy of LGKCGAN-TL model was observed to be higher compared to existing methods [1] and [2]. Let us consider first iteration involving 100 images from Parkinson's Drawings dataset, the accuracy using the LGKCGAN-TL model was found to be 0.98. Subsequently, 0.93 and 0.91 of accuracy were observed by applying [1] and [2], respectively. Similarly, Let us consider first iteration involving 100 images from Dermnet dataset, the accuracy using the LGKCGAN-TL model was found to be 0.97. Subsequently, 0.93 and 0.90 of accuracy were observed by applying [1] and [2], respectively. Multiple runs were carried out for each method with various numbers of input images. The performance outcomes of LGKCGAN-TL model were compared to the results of existing methods. The overall comparison result indicates that the LGKCGAN-TL model increased stroke prediction accuracy by 5% compared to [1] and 8% compared to [2] by applying a Parkinson's Drawings dataset as well as Dermnet dataset.

The LGKCGAN-TL model utilizes Rosenthal correlation analysis in the fully connected dense layer of the transformer learning model to analyze the extracted features from the spiral images in the Parkinson's Drawings dataset. Based on this analysis, spiral patterns that deviate more from normal are identified as indicative of stroke, while others are classified as normal. In the case of the Dermnet dataset, Rosenthal correlation analysis is applied to the extracted features from skin images of patients to assess stroke risk. This analysis provides stroke risk prediction outcomes by classifying Psoriasis, Eczema, and Lupus disease from the images. These outcomes are used to improve the accuracy of the LGKCGAN-TL model for both datasets.

Table 5 Precision

Number of images	Precision using Parkinson's Drawings dataset			Precision using Dermnet dataset		
	LGKCGAN-TL	GA-BiLSTM	DCNN	GKCGAN-TL	GA-BiLSTM	DCNN
100	0.988	0.963	0.951	0.988	0.964	0.940
200	0.985	0.96	0.95	0.986	0.963	0.938
300	0.986	0.968	0.945	0.985	0.971	0.942
400	0.988	0.961	0.948	0.987	0.965	0.945
500	0.987	0.959	0.947	0.988	0.962	0.938

600	0.986	0.962	0.943	0.987	0.967	0.942
700	0.987	0.955	0.947	0.988	0.958	0.941
800	0.985	0.967	0.95	0.987	0.965	0.947
900	0.978	0.968	0.948	0.982	0.966	0.933
1000	0.982	0.961	0.942	0.983	0.965	0.941

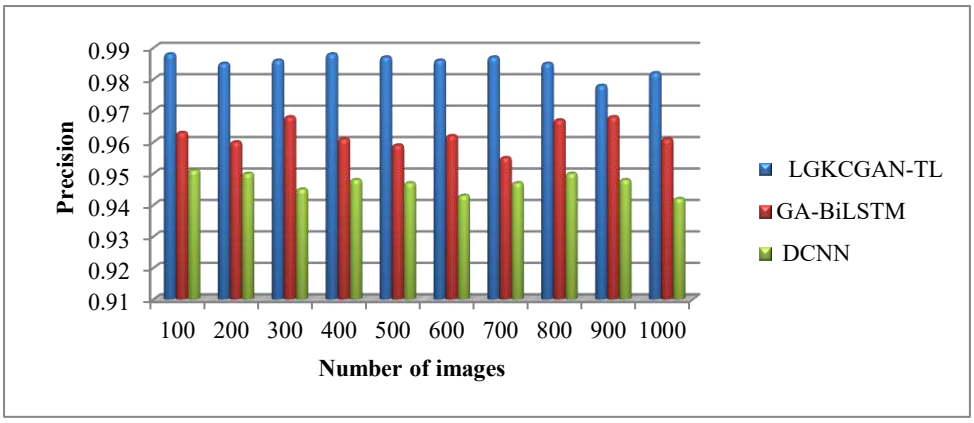


Figure 12 performance results of precision using Parkinson's Drawings dataset

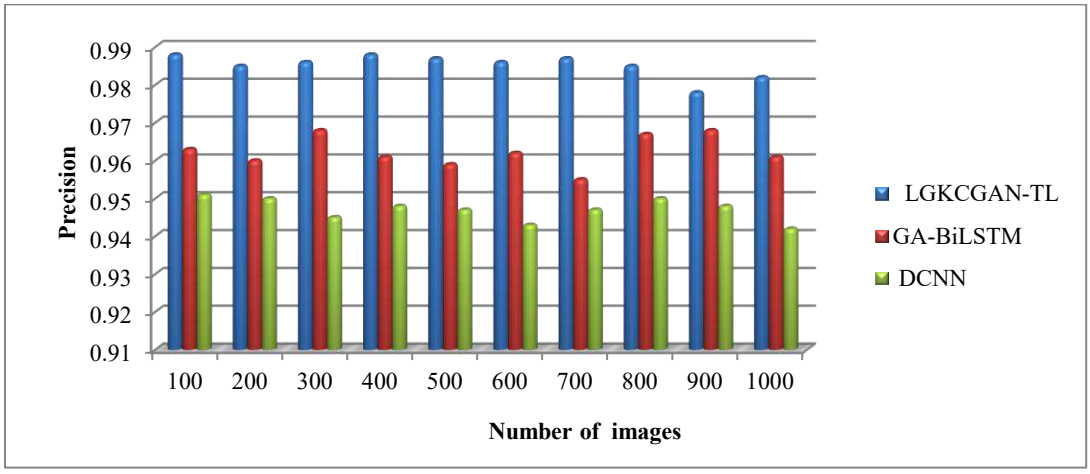


Figure 13 performance results of precision using Dermnet dataset

Figure 12 and 13 illustrates a performance analysis of precision in stroke detection versus the number of images taken in the range from 100 to 1000. The graph depicts the number of input images on the 'x' axis and the precision performance observed on the 'y' axis. Among the three methods, LGKCGAN-TL model shows the improved precision performance compared to the other two existing methods [1] [2]. This improvement is achieved due to the analysis of extracting

feature vector and testing feature vector using Rosenthal correlation function. These features analyses contribute to minimize false positives in stroke prediction and increasing the true positives results. On average, the comparison of ten results reveals that the precision performance during stroke prediction of LGKCGAN-TL model was increased by 2% compared to [1] and 4% compared to [2] by using Parkinson's Drawings dataset. The comparison of ten results reveals that the precision performance during stroke prediction of LGKCGAN-TL model was increased by 2% compared to [1] and 5% compared to [2] by using Dermnet dataset.

Table 6 Recall

Number of images	Recall using Parkinson's Drawings dataset			Recall using Dermnet dataset		
	LGKCGAN-TL	GA-BiLSTM	DCNN	LGKCGAN-TL	GA-BiLSTM	DCNN
100	0.988	0.952	0.940	0.976	0.952	0.940
200	0.983	0.952	0.945	0.975	0.955	0.932
300	0.982	0.957	0.933	0.974	0.952	0.938
400	0.986	0.959	0.936	0.965	0.954	0.937
500	0.974	0.952	0.937	0.975	0.948	0.94
600	0.978	0.96	0.929	0.977	0.953	0.937
700	0.98	0.95	0.937	0.978	0.952	0.933
800	0.978	0.957	0.932	0.973	0.947	0.932
900	0.972	0.955	0.93	0.975	0.955	0.941
1000	0.975	0.953	0.937	0.974	0.951	0.937

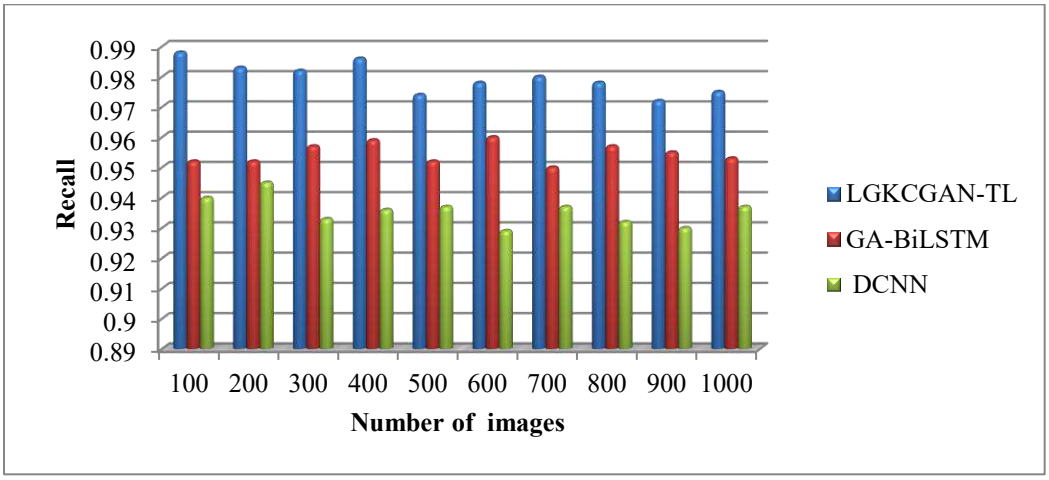


Figure 14 performance results of recall using Parkinson's Drawings dataset

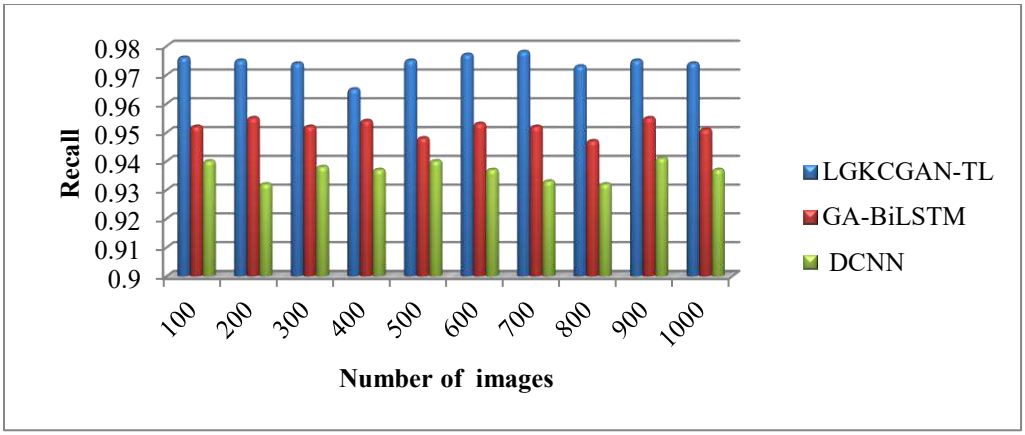


Figure 15 performance results of recall using Dermnet dataset

Figure 14 and 15 illustrates the performance outcomes of recall against the number of images, ranging from 100 to 1000 taken from two datasets. To calculate recall, three methods were employed namely LGKCGAN-TL model, the existing GA-BiLSTM [1], and DCNN [2]. The horizontal axis indicates the number of images, while the vertical axis indicates recall. The experimental results demonstrate that the LGKCGAN-TL model achieved improved recall compared to the other two existing deep learning techniques. For each method, a variety of results were observed with different counts of images. The observed results of the LGKCGAN-TL model were compared with the existing deep learning techniques. The overall comparison shows that the performance of recall using LGKCGAN-TL model in accurately predicting the stroke is enhanced by 3% compared to [1] and 5% compared to [2] by applying the Parkinson's Drawings dataset. Similarly, the overall results shows that the performance of recall using LGKCGAN-TL model is enhanced by 2% compared to [1] and 4% compared to [2] respectively.

Table 7 F1 score

Number of images	F1 score using Parkinson's Drawings dataset			F1 score using Dermnet dataset		
	LGKCGAN-TL	GA-BiLSTM	DCNN	LGKCGAN-TL	GA-BiLSTM	DCNN
100	0.988	0.957	0.945	0.981	0.957	0.94
200	0.984	0.955	0.947	0.980	0.958	0.934
300	0.984	0.962	0.938	0.979	0.961	0.939
400	0.987	0.959	0.941	0.975	0.959	0.940
500	0.980	0.955	0.941	0.981	0.954	0.938
600	0.981	0.960	0.935	0.981	0.959	0.939
700	0.983	0.952	0.941	0.982	0.954	0.936
800	0.981	0.961	0.940	0.979	0.955	0.939
900	0.974	0.961	0.938	0.978	0.960	0.936

1000	0.978	0.956	0.939	0.978	0.957	0.938

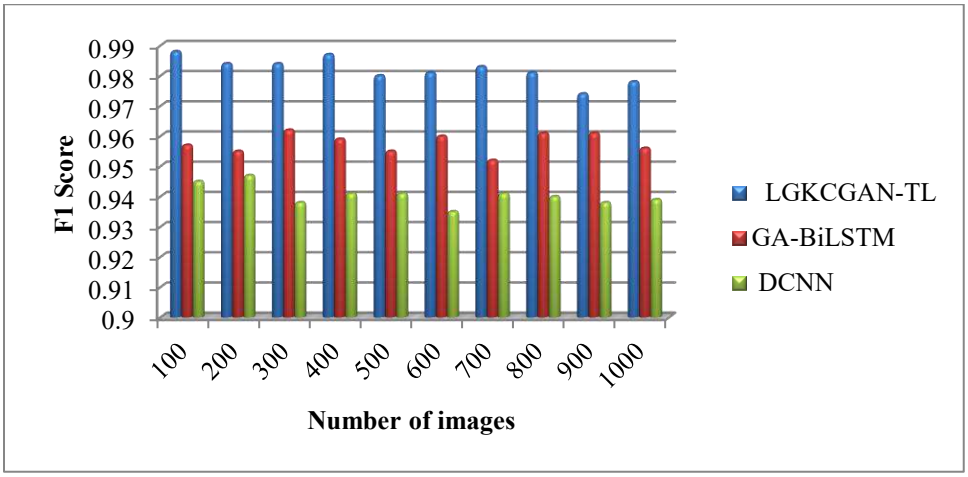


Figure 16 performance results of F1 score using Parkinson's Drawings dataset

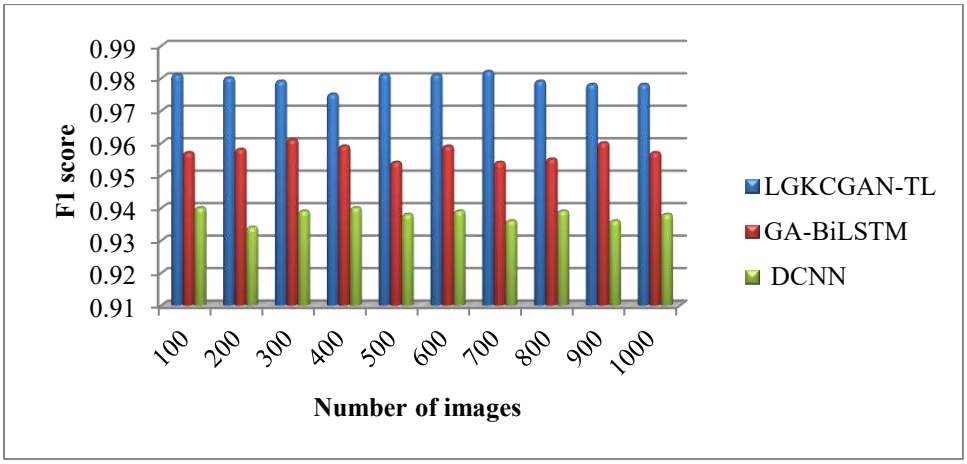


Figure 17 performance results of F1 score using Dermnet dataset

Figures 16 and 17 shows the performance outcomes of the F1-score with respect to different number of images ranged from 100 to 1000. According to the obtained results, the proposed LGKCGAN-TL model demonstrated improved F1-score performance in stroke prediction compared to existing deep learning models. Ten outcomes were obtained for each method. The results of the LGKCGAN-TL model were then compared to existing methods. The average of the ten comparisons showed that the F1-score using the LGKCGAN-TL model improved by 3% and 4% compared to [1] and [2], respectively, when applied to the Parkinson's Drawings dataset. Additionally, the average of the ten comparisons showed that the F1-score using

the LGKCGAN-TL model improved by 2% and 4% compared to [1] and [2], respectively, when applied to the Dermnet dataset.

Table 8 Specificity

Number of images	Specificity using Parkinson's Drawings dataset			Specificity using Dermnet dataset		
	LGKCGAN-TL	GA-BiLSTM	DCNN	LGKCGAN-TL	GA-BiLSTM	DCNN
100	0.937	0.812	0.75	0.928	0.8	0.687
200	0.938	0.835	0.745	0.925	0.822	0.675
300	0.933	0.842	0.755	0.927	0.845	0.685
400	0.935	0.855	0.802	0.931	0.826	0.71
500	0.933	0.863	0.785	0.928	0.844	0.72
600	0.934	0.875	0.745	0.93	0.863	0.715
700	0.932	0.865	0.756	0.928	0.845	0.689
800	0.928	0.825	0.732	0.931	0.824	0.705
900	0.93	0.845	0.765	0.929	0.821	0.675
1000	0.932	0.825	0.785	0.927	0.815	0.668

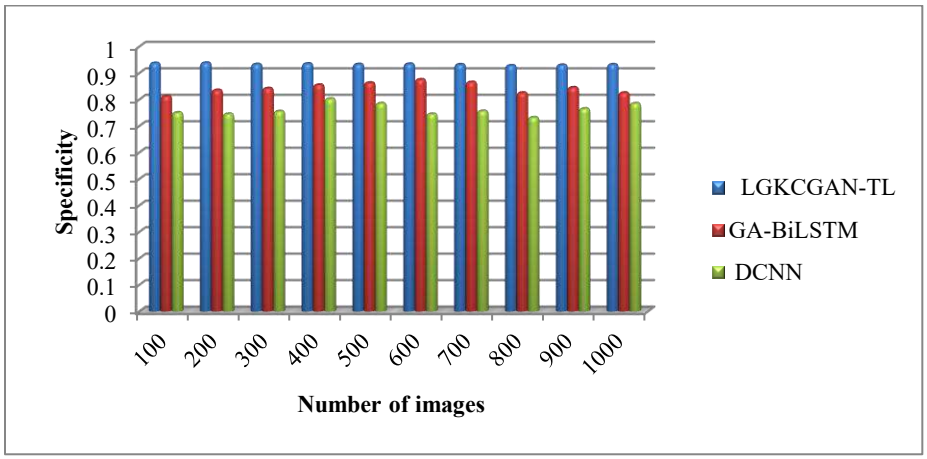


Figure 18 performance results of specificity using Parkinson's Drawings dataset

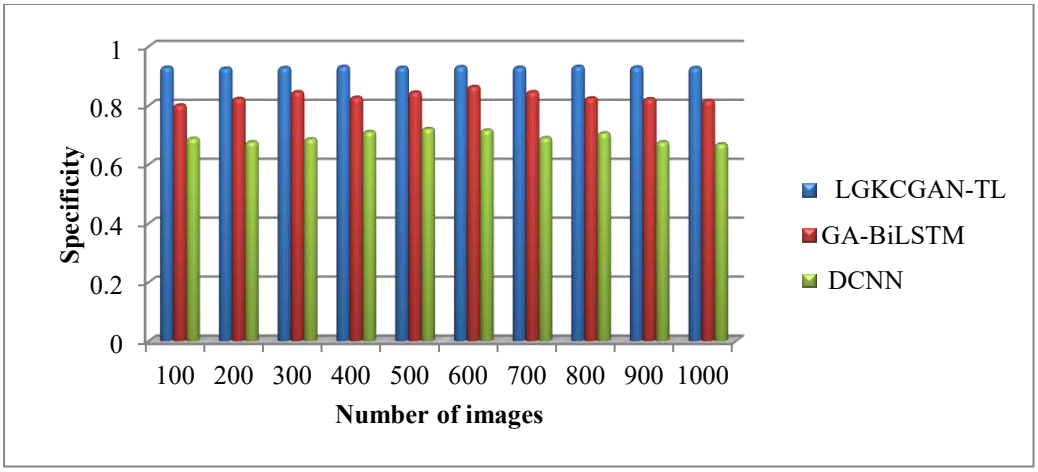


Figure 19 performance results of specificity using Dermnet dataset

Figures 18 and 19 illustrate the performance analysis of specificity against the number of images, ranging from 100 to 1000, taken from two datasets. The horizontal axis represents the number of images, while the vertical axis represents specificity. The experimental results demonstrate that the LGKCGAN-TL model achieved higher specificity compared to two other existing deep learning techniques. Various results were observed for each method with different numbers of images in accurately predicting strokes. The overall results show that the LGKCGAN-TL model increases specificity by 11% compared to [1] and 34% compared to [2] when applied to the Parkinson's drawings dataset. Similarly, the LGKCGAN-TL model increases specificity by 12% compared to [1] and 34% compared to [2] when applied to the Dermnet dataset.

Table 9 Stroke prediction time

Number of images	Stroke prediction time using Parkinson's Drawings dataset			Stroke prediction time using Dermnet dataset		
	LGKCGAN-TL	GA-BiLSTM	DCNN	LGKCGAN-TL	GA-BiLSTM	DCNN
100	28	32	37	30	34	40
200	32.2	35.5	40.5	34.5	37	43.5
300	35.4	38	42.6	38.5	40.2	45.7
400	40.5	42.6	45.8	42	45.8	50
500	42.2	46.2	50	45.5	48.6	53
600	44.5	48.3	53.7	48.8	51.5	55.8
700	46.8	51.5	55.4	50	53.6	58.2
800	48.5	53.4	58.4	52.6	55	60
900	51.2	55.7	60	54.5	58.5	62.4
1000	55	58	61.3	57	60	63.8

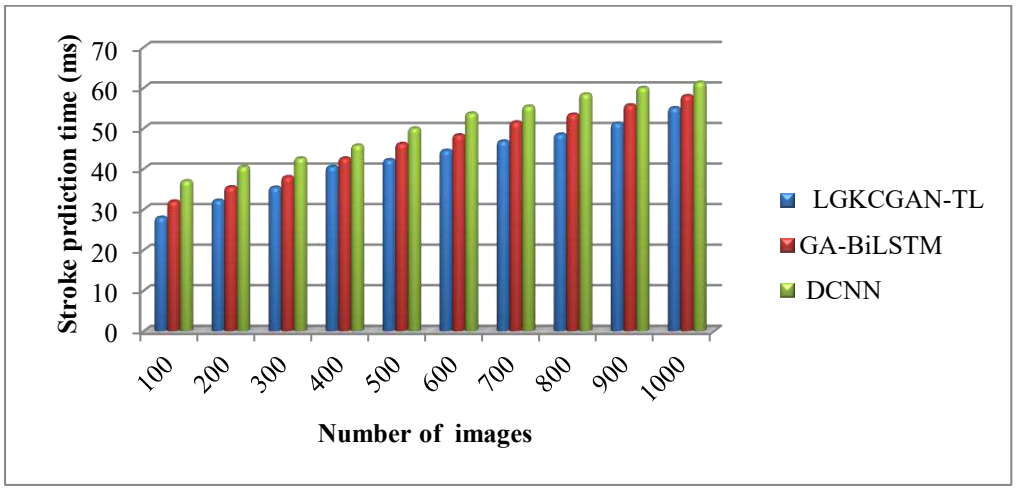


Figure 20 performance results of Stroke prediction time using Parkinson's Drawings dataset

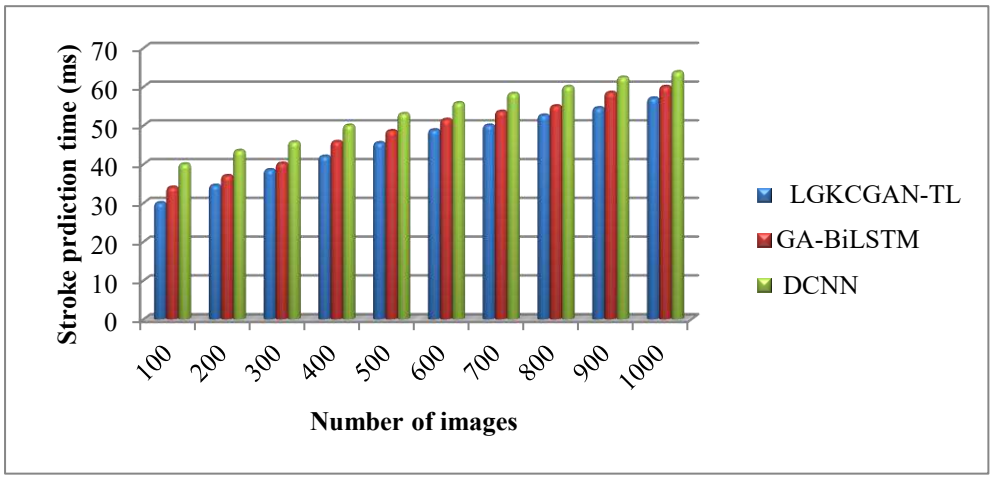


Figure 21 performance results of Stroke prediction time using Dermnet dataset

Figure 20 and 21 illustrates the performance analysis of stroke prediction time using three methods namely LGKCGAN-TL model, the existing GA-BiLSTM [1], and DCNN [2]. For each method, a simulation of 10 runs was performed with 1000 distinct images collected from two dataset. From the above figure, increasing the number of images, the time incurred for stroke prediction was also found to be increased. However, the stroke prediction time using the LGKCGAN-TL model, was found to be minimized when compared to [1] and [2] respectively.

The reason behind this is to perform image patch embedding and position embedding as well as feature extraction in the transformer learning model. For each patch of image in the preprocessed images, the features of image patches are extracted. Consequently, these features are analyzed by applying a Rosenthal correlation function. This process minimizes the stroke prediction time from the given input image. The overall results indicate that the stroke prediction time of the LGKCGAN-TL model is considerably minimized by 8% and 16% compared to [1] and [2], respectively when applying a Parkinson's Drawings dataset and 7% and 15% when compared to [1] and [2], when applying a Dermnet dataset.

5.1 Confusion matrix

A confusion matrix is a tool commonly used in classification to assess the performance of a proposed LGKCGAN-TL model. It provides a summary of prediction results by comparing the actual (true) labels with the predicted labels generated by the model.

	Total images 1000	**Actual value**		
		Positive	**Negative**	
Predicted value	**Positive**	TP=825	FP=50	875
	Negative	FN=25	TN=100	125
		850	150	

Table 10 Confusion metrics using LGKCGAN-TL model using Parkinson's Drawings dataset

As shown in table 10, the confusion matrix of the proposed LGKCGAN-TL model is presented using Parkinson's Drawings dataset of 1000 images. The LGKCGAN-TL model achieved 825 true positives (TP) and 100 true negatives (TN), with 50 false positives (FP) and 25 false negatives (FN).

Total instances 1000	**Actual value**	
	Positive	**Negative**

Predicted value	**Positive**	TP=820	FP=55	875
	Negative	FN=30	TN=95	125
		850	150	

Table 11 Confusion metrics using LGKCGAN-TL model using Dermnet dataset

As shown in table 11, the confusion matrix of the proposed LGKCGAN-TL model is presented using Dermnet dataset of 1000 images. The LGKCGAN-TL model achieved 820 true positives (TP) and 95 true negatives (TN), with 55 false positives (FP) and 30 false negatives (FN).

5.2 Performance of ROC curve

The ROC (Receiver Operating Characteristic) curve evaluates the performance of a LGKCGAN-TL model for positive class prediction. It plots the True Positive Rate (TPR) against the False Positive Rate (FPR) in Table 12.

Table 12 Tabulation for ROC curve

FPR	**TPR**		
	LGKCGAN-TL	**GA-BiLSTM**	**DCNN**
0.1	0.11	0.09	0.07
0.2	0.3	0.25	0.2
0.3	0.46	0.38	0.3
0.4	0.61	0.5	0.4
0.5	0.71	0.58	0.52
0.6	0.8	0.68	0.62
0.7	0.88	0.78	0.7
0.8	0.95	0.85	0.8
0.9	0.98	0.9	0.86
1	0.99	0.94	0.91

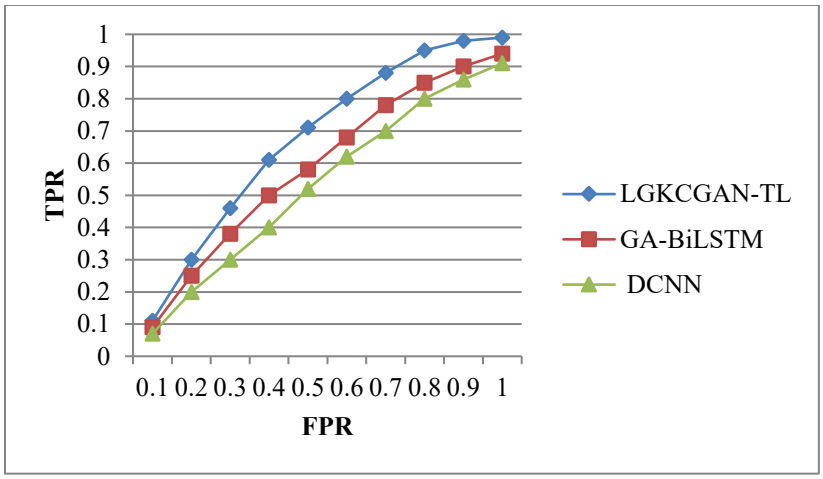


Figure 22 performance results of ROC curve

Figure 22 depicts the ROC curve analysis comparing the proposed LGKCGAN-TL model with two existing methods, GA-BiLSTM [1], and DCNN [2]. In this graph, the x-axis represents the false positive rate (FPR), while the y-axis represents the true positive rate (TPR). The ROC curve assesses stroke disease prediction based on these rates. From the figure, it is clear that the LGKCGAN-TL model outperforms the existing methods in stroke disease prediction.

5.3 Discussion

The experimental findings show that the proposed LGKCGAN-TL model can significantly enhance performance of the early-stage stroke prediction in comparison with the other baseline models GA-BiLSTM and DCNN. This is primarily due to the addition of image preprocessing, GAN-based augmentation, and transformer-based feature learning to a single architecture. The index box linear denoising of the Camargo is beneficial as it minimizes the noise artifacts of the medical image which maximizes the Peak Signal-to-Noise Ratio (PSNR) and boosts the quality of the input data to be used in subsequent analysis. The proposed method, therefore, delivered about 8-9% better PSNR as compared to the compared models when it was tested against both Parkinson and Dermnet datasets as well.

The other aspect that has led to the better performance is the implementation of Gaussian kernel Cycle Generative Adversarial Network to augment the data. This method will produce more realistic samples and will deal with the fact that training data is limited and the model generalizes better. By increasing the size of the dataset up to 1000 training images, the proposed model could have learned the representations of features richer, thus, achieving better classification results. The experimental findings display that the model attained an average accuracy of approximately 98 99

which is higher than the GA-BiLSTM and DCNN models by approximately 5 and 8 percent, respectively.

Moreover, the module of learning that correlated transformer is important in acquiring the intricate spatial associations and long-range correlation between patches in an image. In comparison to traditional convolutional networks, the transformer-based architecture employs the self-attention mechanism to learn the global contextual data of the drawing patterns and dermatological images in Parkinson and convert it into data. This allows the system to successfully determine disease related trends related to stroke risk. As a result, the proposed model was more precise (0.98), recall (0.97-98) and F1-score (0.98) as compared to the current techniques, meaning it was considered a more reliable classification.

The effectiveness of the proposed approach is also supported with the help of the confusion matrix and ROC analysis. The model properly identified 825 true positive and 100 true negative cases among 1000 samples in the Parkinson dataset, which shows that the model has a high diagnostic ability. Additionally, the ROC curve demonstrates a greater true positive rate at the various levels of false positive rates, which means that it is more predictive. The proposed model also minimized the stroke prediction time (about 7-16) as well as this is primarily because of the effective feature extraction by transformer-based patch embeddings.

All in all, the findings suggest that a hybrid approach of complex preprocessing, augmentation with GANs, and the use of transformer-based learning could serve as an effective model of early stroke detection. The multimodal disease indicators covered in the proposed model via the Parkinson disease and dermatological conditions are effective in terms of capturing the disease indicators that can be used to make better predictive accuracy and to make decisions faster in clinical applications.

6. CONCLUSION

The study introduced a new LGKCGAN-TL model to predict stroke in the early stages based on the drawings of Parkinson and images of skin diseases. The proposed structure combines index box linear denoising, Camargo, with CycleGAN-based data augmentation using a Gaussian kernel and connected to a learning correlative transformer to improve the accuracy of prediction and decrease the computation time. The results of the experimental assessment of the use of Parkinson’s Drawings and Dermnet datasets allowed showing significant performance improvement on a set of indicators. The maximum accuracy of the proposed model was 0.99,

precision of 0.988, recall of 0.988 and F1-score of 0.988 and specificity of 0.937. The preprocessing technique also enhanced PSNR up to 816 percent and the transformer-based feature analysis decreased the stroke prediction time to almost 816 percent as compared with the current GA-BiLSTM and DCNN models. The outcome of confusion matrix also supported the efficacy of the model with 825 correct positives and 100 correct negatives on the Parkinson dataset and 820 correct positives and 95 correct negatives on the Dermnet dataset. In general, the LGKCGAN-TL model is capable of identifying the risks of stroke and estimating them correctly and efficiently due to the presence of neurological and dermatological markers. Nonetheless, the current study possesses some limitations including dependence on a small number of datasets and lack of multimodal clinical evidence including MRI, CT scans, and health records of patients. It is possible to expand the model in future work with larger multi-institutional datasets, multimodal medical imaging, and clinical parameters and apply federated or real-time frames of the IoMT to enhance the strength, scalability and feasibility of early stroke prediction systems further.

Compliance with Ethical Standards

Conflict of interest

The authors declare that they have no conflict of interest.

Human and Animal Rights

This article does not contain any studies with human or animal subjects performed by any of the authors.

Informed Consent

Informed consent does not apply as this was a retrospective review with no identifying patient information.

Funding: Not applicable
Conflicts of interest Statement: Not applicable
Consent to participate: Not applicable
Consent for publication: Not applicable

Availability of data and material:

Data sharing is not applicable to this article as no new data were created or analyzed in this study.
Code availability: Not applicable

REFERENCES

[1] Muhammad Asim Saleem, Ashir Javeed , Wasan Akarathanawat, Aurauma Chutinet, Nijasri Charnnarong Suwanwela , Widhyakorn Asdornwised , Surachai Chaitusaney , Sunchai Deelertpaiboon, Wattanasak Srisiri, "Innovations in Stroke Identification: A Machine Learning-Based Diagnostic Model Using Neuroimages", IEEE Access, Volume 12, 2024, Pages 35754 – 35764. **DOI:** 10.1109/ACCESS.2024.3369673

[2] Sanaz Nazari-Farsani, Yannan Yu, Rui Duarte Armindo, Maarten Lansberg, David S. Liebeskind, Gregory Albers, Soren Christensen, Craig S. Levin, Greg Zaharchuk, "Predicting final ischemic stroke lesions from initial diffusion-weighted images using a deep neural network", NeuroImage: Clinical, Elsevier, Volume 37, 2023, Pages 1-10. https://doi.org/10.1016/j.nicl.2022.103278

[3] Francesco Pacchiano, Mario Tortora, Sabrina Criscuolo, Katya Jaber, Pasquale Acierno, Marta De Simone, Fabio Tortora, Francesco Briganti & Ferdinando Caranci, "Artificial intelligence applied in acute ischemic stroke: from child to elderly", La radiologia medica, Springer, Volume 129, 2024, Pages 83–92. https://doi.org/10.1007/s11547-023-01735-1

[4] Yumei Liu, Li Xue, Yingying Zhang, Anmu Xie, "Association between Stroke and Parkinson's Disease: a Meta-analysis", Journal of Molecular Neuroscience, Springer, Volume 70, 2020, Pages 1169–1176. https://doi.org/10.1007/s12031-020-01524-9

[5] Jasjit S. Suri, Sudip Paul, Maheshrao A. Maindarkar, Anudeep Puvvula, Sanjay Saxena, Luca Saba, Monika Turk, John R. Laird, Narendra N. Khanna, Klaudija Viskovic, Inder M. Singh, Mannudeep Kalra, Padukode R. Krishnan, Amer Johri, and Kosmas I. Paraskevas, "Cardiovascular/Stroke Risk Stratification in Parkinson's Disease Patients Using Atherosclerosis Pathway and Artificial Intelligence Paradigm: A Systematic Review", Metabolites, Volume 12(, Issue 4, 2022, Pages 1-30. DOI: 10.3390/metabo12040312

[6] Eui-Sun Kim, Ji-Min Heo, Sung-Jong Eun, Jun Young Lee, "Development of Early-Stage Stroke Diagnosis System for the Elderly Neurogenic Bladder Prevention", International Neurourology Journal, Volume 26, Pages 76-82. DOI: 10.5213/inj.2244030.015

[7] Mohammed F. Allebawi, Thameur Dhieb, Mohamed Neji, Nouha Farhat, Emna Smaoui, Tarek M. Hamdani, Mariem Damak, Chokri Mhiri, Bilel Neji, Taha Beyrouthy, And Adel M. Alimi, "Parkinson's Disease Detection From Online Handwriting Based on Beta-Elliptical Approach and

Fuzzy Perceptual Detector", IEEE Access, Volume 12, 2024, Pages 56936 – 56950. **DOI:** 10.1109/ACCESS.2024.3387342

[8] Haisheng Hui , Xueying Zhang , Fenglian Li , Xiaobi Mei , And Yuling Guo, "A Partitioning-Stacking Prediction Fusion Network Based on an Improved Attention U-Net for Stroke Lesion Segmentation", IEEE Access, Volume 8, 2020, Pages 47419 – 47432. **DOI:** 10.1109/ACCESS.2020.2977946

[9] Adriano Pinto, Joana Amorim, Arsany Hakim, Victor Alves, Mauricio Reyes, And Carlos A. Silva, "Prediction of Stroke Lesion at 90-Day Follow-Up by Fusing Raw DSC-MRI With Parametric Maps Using Deep Learning", IEEE Access , Volume 9, 2021, Pages 26260 – 26270. **DOI:** 10.1109/ACCESS.2021.3058297

[10] Jesus A Perdomo-Lampignano, Tiberiu A Pana, Isobel Sleeman, Allan B Clark, Kittisak Sawanyawisuth, Somsak Tiamkaoand Phyo K Myint, "Parkinson's disease and patient related outcomes in stroke: A matched cohort study", Journal of Stroke and Cerebrovascular Diseases, Elsevier, Volume 29, Issue 7, 2020, Pages 1-8. https://doi.org/10.1016/j.jstrokecerebrovasdis.2020.104826

[11] Dorji Harnod, Tomor Harnod, Cheng-Li Lin, Chung Y. Hsu, Chia-Hung Kao, "Poststroke Parkinsonism associates with an increased mortality risk in patients", Annals of Translational Medicine, Volume 8, issue 7, 2020, DOI : 10.21037/atm.2020.03.90

[12] Hea Lim Choi, Jong Hyeon Ahn, Won Hyuk Chang, Wonyoung Jung, Bong Sung Kim, Kyungdo Han ,Jinyoung Youn, Dong Wook Shin, "Risk of Parkinson disease in stroke patients: A nationwide cohort study in South Korea", European Journal of Neurology, Wiley, Volume 31, Issue 4, 2024, Pages 1-8.

[13] Mandeep Kaur, Sachin R. Sakhare, Kirti Wanjale, Farzana Akter, "Early Stroke Prediction Methods for Prevention of Strokes", Behavioural Neurology, Hindawi, Volume 2022, April 2022, Pages 1-9. **https://doi.org/10.1155/2022/7725597**

[14] Tahia Tazin , Md Nur Alam, Nahian Nakiba Dola, Mohammad Sajibul Bari, Sami Bourouis , and Mohammad Monirujjaman Khan, "Stroke Disease Detection and Prediction Using Robust

Learning Approaches", Journal of Healthcare Engineering , Hindawi, Volume 2021, November 2021, Pages 1-12. https://doi.org/10.1155/2021/7633381

[15]Soumyabrata Dev, Hewei Wang, Chidozie Shamrock Nwosu, Nishtha Jain, Bharadwaj Veeravalli, Deepu John, "A predictive analytics approach for stroke prediction using machine learning and neural networks", Healthcare Analytics, Elsevier, Volume 2, 2022, Pages 1-9. https://doi.org/10.1016/j.health.2022.100032

[16] Tak Sung Heo, Yu Seop Kim, Jeong Myeong Choi, Yeong Seok Jeong, Soo Young Seo, Jun Ho Lee, Jin Pyeong Jeon and Chulho Kim, "Prediction of Stroke Outcome Using Natural Language Processing-Based Machine Learning of Radiology Report of Brain MRI", Journal of personalized medicine, Volume 10, Issue 4, 2020, Pages ; https://doi.org/10.3390/jpm10040286

[17] Phongphan Phienphanich, Nichapa Lerthirunvibul, Ekabhat Charnnarong, Adirek Munthuli, Charturong Tantibundhit, And Nijasri C. Suwanwela, "Generalizing a Small Facial Image Dataset Using Facial Generative Adversarial Networks for Stroke's Facial Weakness Screening", IEEE Access , Volume 11, 2023, Pages 64886 – 64896. **DOI:** 10.1109/ACCESS.2023.3287389

[18] Tongan Cai, Haomiao Ni, Mingli Yu, Xiaolei Huang, Kelvin Wong, John Volpi, James Z. Wang, Stephen T.C. Wong, "DeepStroke: An Efficient Stroke Screening Framework for Emergency Rooms with Multimodal Adversarial Deep Learning", Medical Image Analysis, Elsevier, Volume 80, 2022, Pages 1-18. https://doi.org/10.1016/j.media.2022.102522

[19] Remah Mutasim Elbashir and Moi Hoon Yap, "Evaluation of Automatic Facial Wrinkle Detection Algorithms", journal of imaging, Volume 6, Issue 4, 2020, Pages 1-10. **https://doi.org/10.3390/jimaging6040017**

[20] Laura Sánchez-Cirera ,Saima Bashir ,Adina Ciscar,Carla Marco,Verónica Cruz,Mikel Terceño,Yolanda Silva,Joaquín Serena, "Prevalence of the Frank's sign by aetiopathogenic stroke subtype: A prospective analysis", Plos one, Volume 16, Issue 12, Pages 1-11. https://doi.org/10.1371/journal.pone.0261080

[21] Venkatesan Rajinikanth, Shabnam Mohamed Aslam and Seifedine Kadry, "Deep Learning Framework to Detect Ischemic Stroke Lesion in Brain MRI Slices of Flair/DW/T1 Modalities", Symmetry, Volume 13, Issue 11, 2021, Pages 1-16. https://doi.org/10.3390/sym13112080

[22] Hossein Abbasi, Maysam Orouskhani, Samaneh Asgari , Sara Shomal Zadeh, “Automatic brain ischemic stroke segmentation with deep learning: A review”, Neuroscience Informatics, Elsevier, Volume 3, Issue 4, 2023, Pages 1-10. https://doi.org/10.1016/j.neuri.2023.100145

[23] Mrs. Anitha Patil and Suresh Kumar Govindaraj, “ADL-BSDF: A Deep Learning Framework for Brain Stroke Detection from MRI Scans towards an Automated Clinical Decision Support System”, International Journal on Recent and Innovation Trends in Computing and Communication, Volume 11, Issue 3, 2023, Pages 11-23. https://doi.org/10.17762/ijritcc.v11i3.6195

[24] Oznur Ozaltin, Orhan Coskun, Ozgur Yeniay and Abdulhamit Subasi, “A Deep Learning Approach for Detecting Stroke from Brain CT Images Using OzNet”, Bioengineering, Volume 9, Issue 12, 2022, Pages 1-16. https://doi.org/10.3390/bioengineering9120783

[25] Weidao Chen, Jiangfen Wu, Ren Wei, Shuang Wu, Chen Xia, Dawei Wang, Daliang Liu, Longmei Zheng, Tianyu Zou, Ruijiang Li, Xianrong Qi & Xiaotong Zhang, “Improving the diagnosis of acute ischemic stroke on non-contrast CT using deep learning: a multicenter study”, Insights into Imaging, Springer, volume 13, 2022, Pages 1-12. https://doi.org/10.1186/s13244-022-01331-3

[26] Wei-Chun Wang , Shang-Yu Chien, Sheng-Ta Tsai, Yu-Wan Yang, Dang-Khoa Nguyen, Ya-Lun Wu, Ming-Kuei Lu , Ting-Hsuan Sun, Jiaxin Yu , Ching-Ting Lin, Chien-Wei Chen, Kai-Cheng Hsu, Chon-Haw Tsai, “Automated delineation of acute ischemic stroke lesions on non-contrast CT using 3D deep learning: A promising step towards efficient diagnosis and treatment’, Biomedical Signal Processing and Control, Elsevier, Volume 93, 2024, Pages 1-11. https://doi.org/10.1016/j.bspc.2024.106139

[27] Lisa Herzog, Elvis Murina, Oliver Dürr, Susanne Wegener, Beate Sick, “Integrating uncertainty in deep neural networks for MRI based stroke analysis”, Medical Image Analysis, Elsevier, Volume 65, 2020, Pages 1-21. https://doi.org/10.1016/j.media.2020.101790

[28] Yi-Chia Wei, Wen-Yi Huang, Chih-Yu Jian, Chih-Chin Heather Hsu, Chih-Chung Hsu, Ching-Po Lin, Chi-Tung Cheng, Yao-Liang Chen, Hung-Yu Wei, KuanFu Chen, “Semantic segmentation guided detector for segmentation, classification, and lesion mapping of acute ischemic stroke in

MRI images", NeuroImage: Clinical, Elsevier, Volume 35, 2022, Pages 1-12. https://doi.org/10.1016/j.nicl.2022.103044

[29] Shatakshi Singh, Dimple Dawar, Esha Mehmood, Jeyaraj Durai Pandian, Rajeshwar Sahonta , Subhash Singla, Amit Batra, Cheruvu Siva Kumar, Manjunatha Mahadevappa, "Determining Diagnostic Utility of EEG for Assessing Stroke Severity using Deep Learning Models", Biomedical Engineering Advances, Elsevier, Volume 7, 2024, Pages 1-11. https://doi.org/10.1016/j.bea.2024.100121

[30] Sanghoon Jeon, Yang-Soo Lee, And Sang Hyuk Son, "Cascade Windows-Based Multi-Stream Convolutional Neural Networks Framework for Early Detecting In-Sleep Stroke Using Wristbands", IEEE Access , Volume 11, 2023, Pages 84944 – 84956. D**OI:** 10.1109/ACCESS.2023.3301872